STATISTICAL PROPERTIES OF THE LARGE SCALE STRUCTURES:

CLUSTER NUMBER COUNTS

For a review: Allen+2011 **or** Kravtsov+2012 or https://arxiv.org/pdf/2505.07697

STRUCTURE FORMATION: DARK MATTER HALOS

In the LCDM scenario, structures grow *hierarchically*: Small overdensities are able to overcome the cosmological expansion and collapse first, and the resulting dark matter "halos" merge together to form larger halos which serve as sites of galaxy and galaxy cluster formation

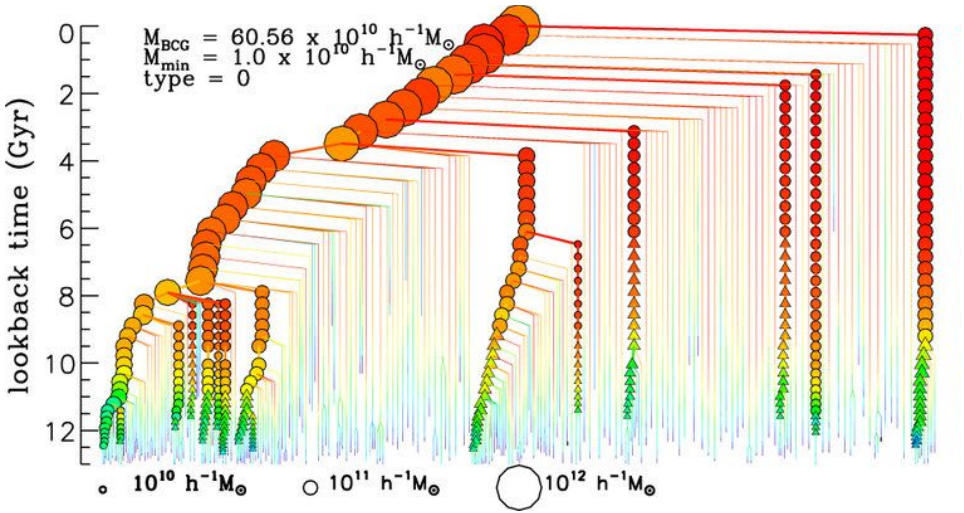

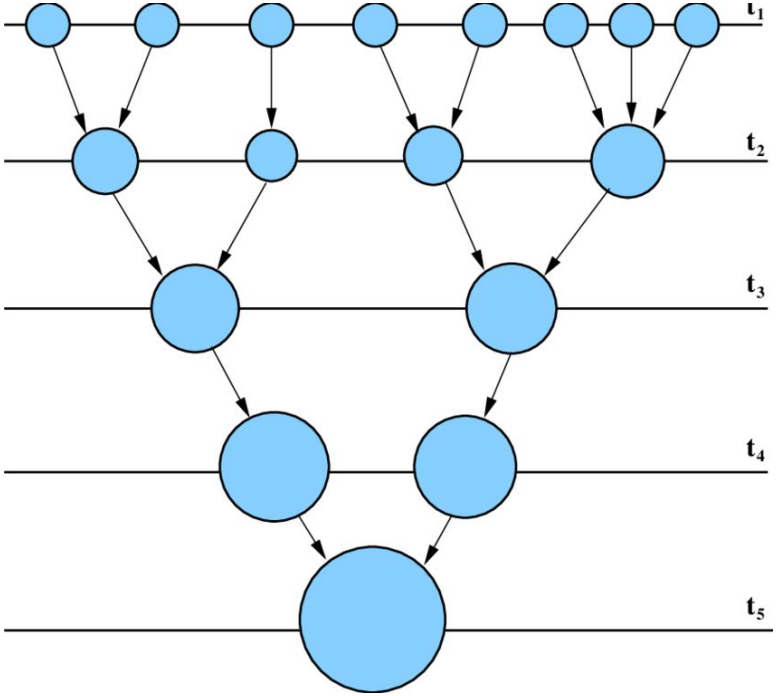

STRUCTURE FORMATION: SPHERICAL COLLAPSE MODEL

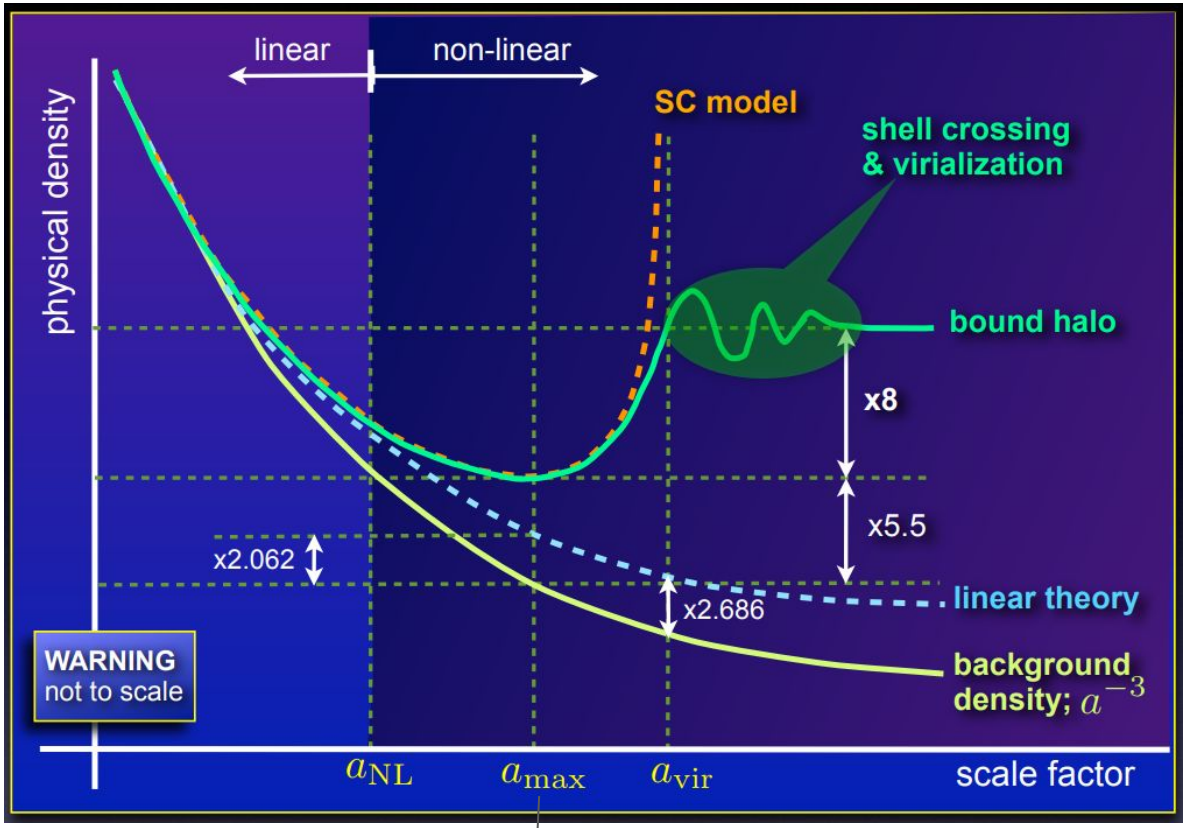

We can follow the collapse of a spherical overdensity in a homogeneous universe.

Expansion ($a < a_{max}$)

$\bar{\rho}_{\rm bkg} \propto a^{-3}$

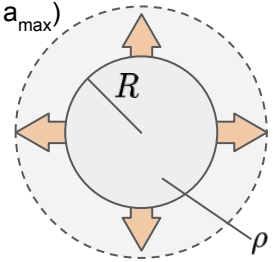

Turn-around ($a=a_{max}$)

$\dot{a} = 0$

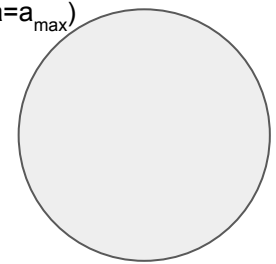

Collapse and Virialization ($a=a_{vir}$)

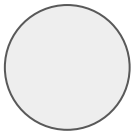

$R(a_{\rm vir}) = R(a_{\rm max})/2 \rightarrow \rho(a_{\rm vir})/\rho(a_{\rm max}) = 8$

See e.g. here

STRUCTURE FORMATION: SPHERICAL COLLAPSE MODEL

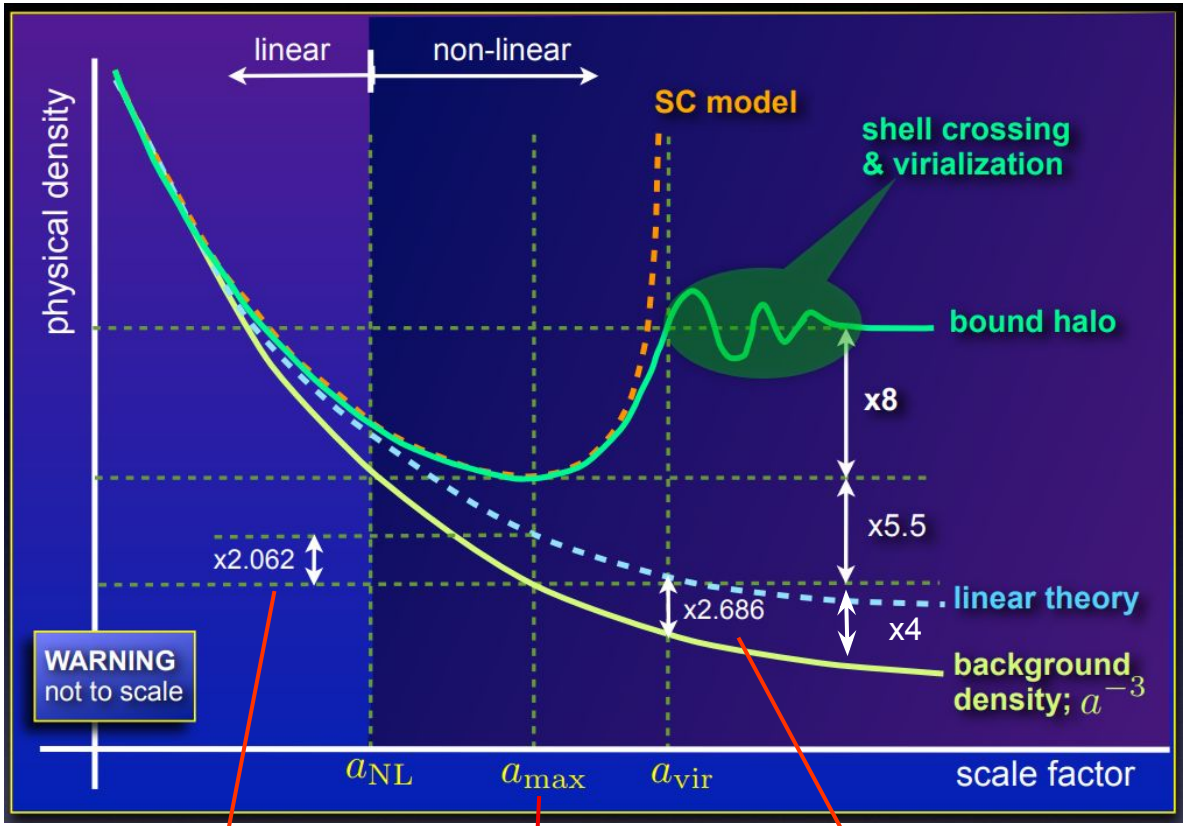

We can follow the collapse of a spherical overdensity in a homogeneous universe. Even if SC model becomes inaccurate shortly after turn-around, it is still a useful model to identify important epochs in the linearly evolved density field.

- The linearly extrapolated density field collapses when $\delta_{\rm lin} = \delta_c = 1.686$
- Virialized dark matter haloes have an average overdensity of $\Delta_{\rm vir} = 178$

STRUCTURE FORMATION: SPHERICAL COLLAPSE MODEL

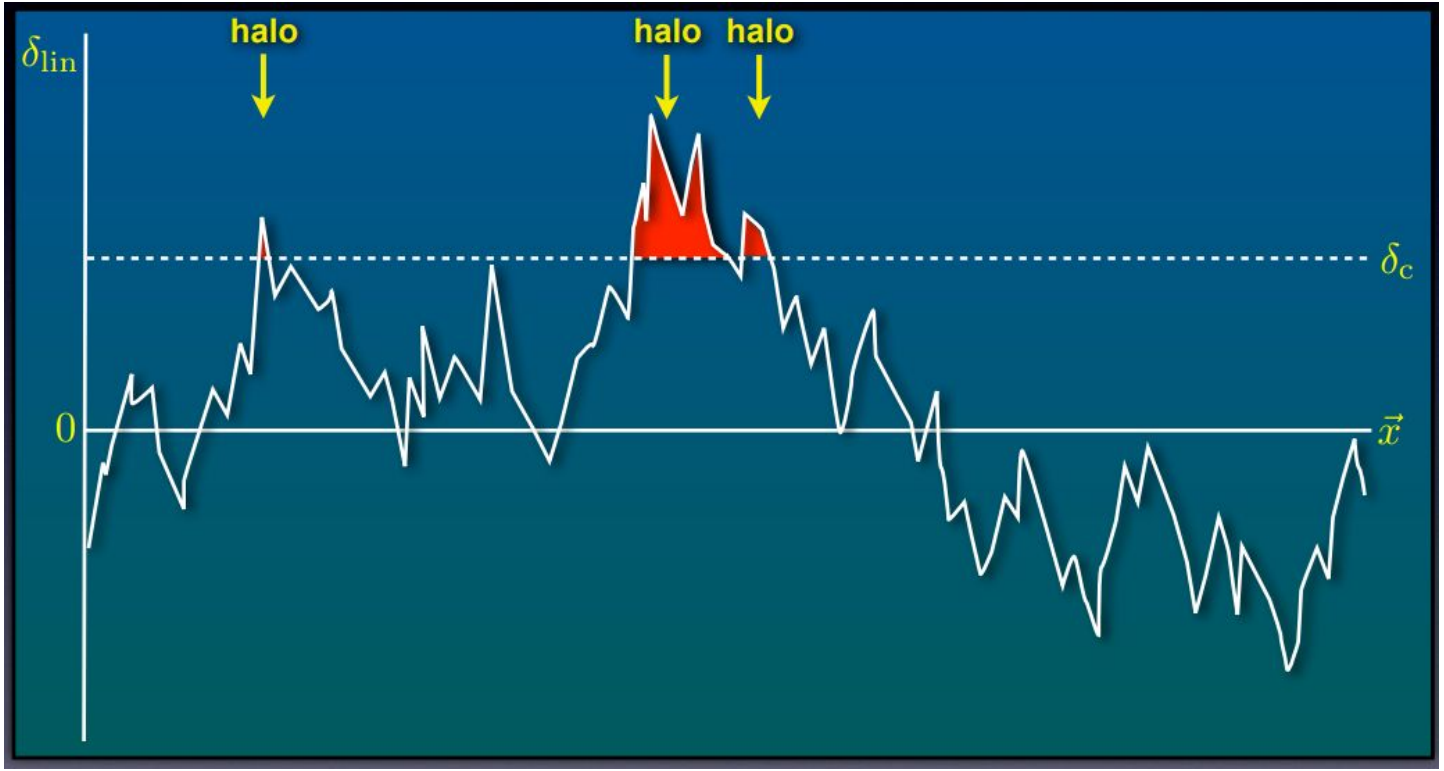

According to the spherical collapse model, regions with $\delta(x,t) > \delta_c \simeq 1.686$ will have collapsed to produce dark matter haloes by time *t.*

Assuming a Gaussian density field, the fraction of cosmic volume with $\delta(x,t) > \delta_c$ depends only on the variance of the matter density field:

$$\sigma^2 = < \delta^2 >$$

GALAXY CLUSTERS

Illustris TNG simulation

Most massive bound objects in the Universe:

- R ≃ 1 - 5 Mpc
- M ≃ 10^{14} - 10^{15} $M_\odot$

DARK MATTER

BARYONS

Multi-component systems:

Galaxies and stars (~5%)

ICM (~15%)

DM (~80%)

OPTICAL

RICHNESS, LENSING EFFECTS

X-RAYS

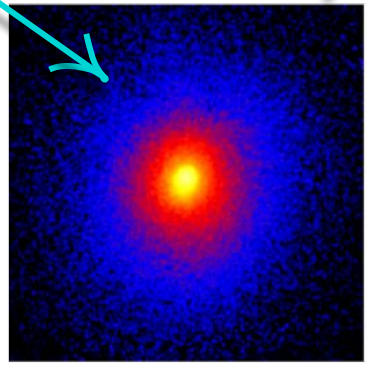

LUMINOUS AND EXTENDED X-RAY SOURCES

MICROWAVES

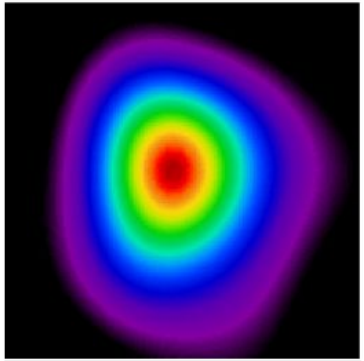

SUNYAEV-ZEL'DOVICH EFFECT

Credit: Allen+11

GALAXY CLUSTERS AS COSMOLOGICAL PROBE

The abundance and spatial distribution of galaxy clusters are sensitive to the growth rate of cosmic structures and expansion history of the Universe

σ_8: Amplitude of the matter power spectrum

Ω_m: Present-day total matter density

$$S_8 = \sigma_8 (\Omega_m / 0.3)^{0.5}$$

Dark energy equation of state parameter *w*
Total neutrino mass
Deviation from GR
….

Evolution of the clusters population in 2 N-body simulations

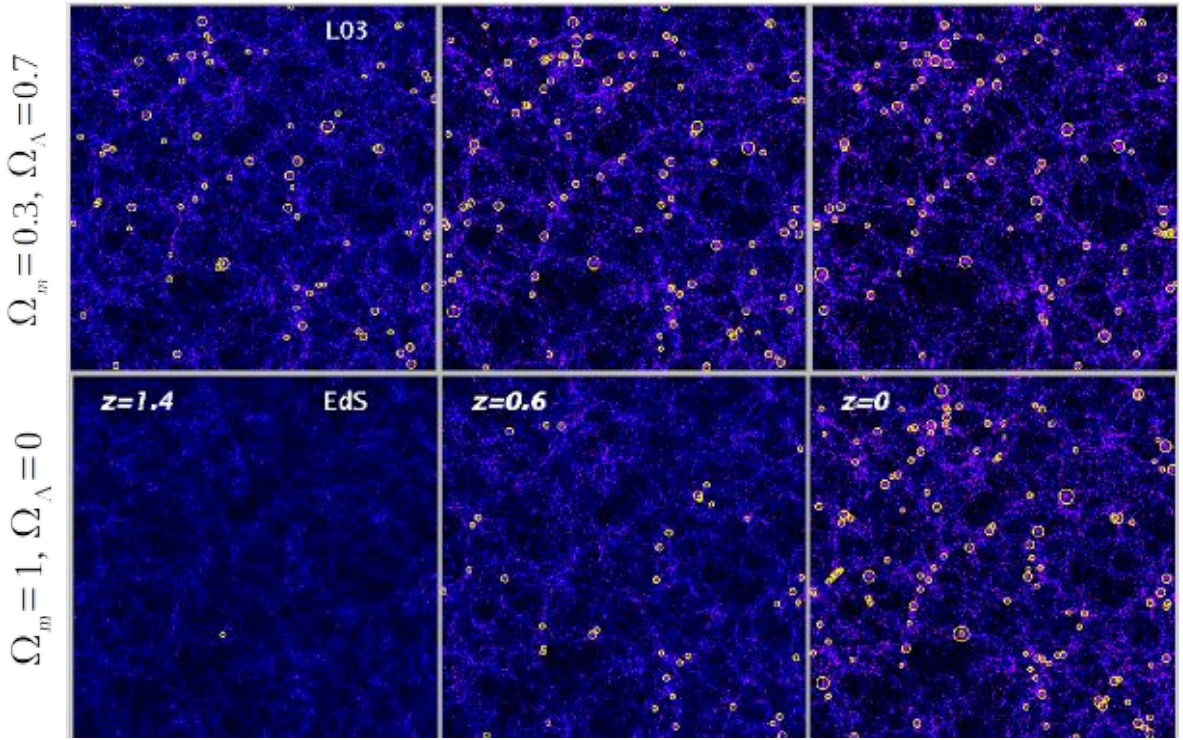

From Borgani, Guzzo 2001

THE HALO MASS FUNCTION

Cluster abundance:

$$\frac{dN}{dzd\Omega} = \frac{dV}{dzd\Omega} n(M,z)$$

geometry

growth

The halo mass function:

$$n(z,M) = \frac{\rho_m}{M} f(\sigma) \frac{d\ln(\sigma^{-1})}{dM}$$

Variance of the density field:

$$\sigma(z,R) = \frac{1}{2\pi^2} \int_0^\infty dk\, k^2 P_m(z,k) |W(kR)|^2$$

Matter power spectrum

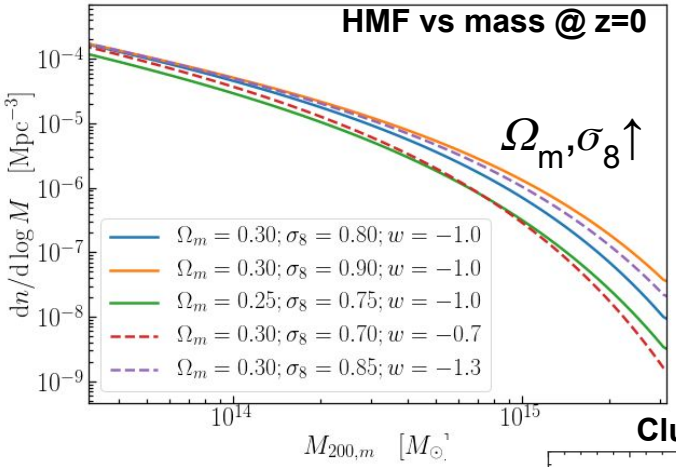

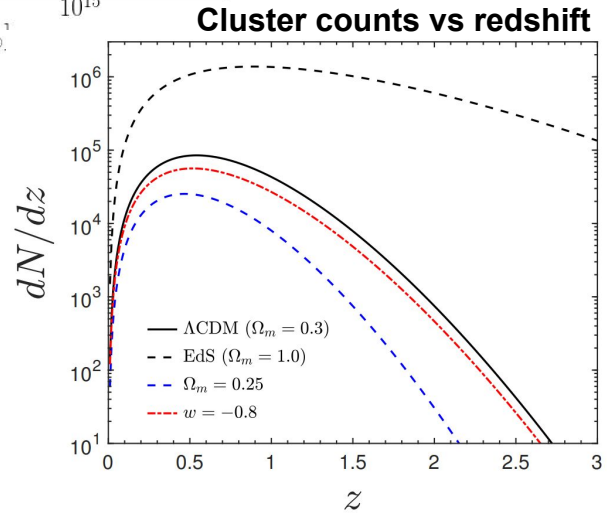

THE HALO MASS FUNCTION: MASSIVE NEUTRINOS

Produced in the early-Universe and kept in thermal equilibrium by weak interactions

Decoupling at T_{dec} = 2 – 4 MeV

$T_{dec} \gg m_\nu \rightarrow$ **ultra-relativistic at decoupling**

Free-streaming length: $\lambda_{fs} \sim \frac{c}{H} = R_H \sim c\,t$

Contribute to the radiation energy content

Non-relativistic transition:

$$(1+z_{nr}) = \frac{1}{a_{nr}} \simeq 2\times 10^3 \left(\frac{m_\nu}{1\,eV}\right)$$

Free-streaming wavenumber:

$$k_{nr} = 2\pi \frac{a_{nr}}{\lambda_{fs}} \simeq 0.018\,\Omega_m^{1/2} \left(\frac{m_\nu}{1\,eV}\right) h\ Mpc^{-1}$$

Contribute to the matter energy content

Evolution of the free-streaming wavenumber:

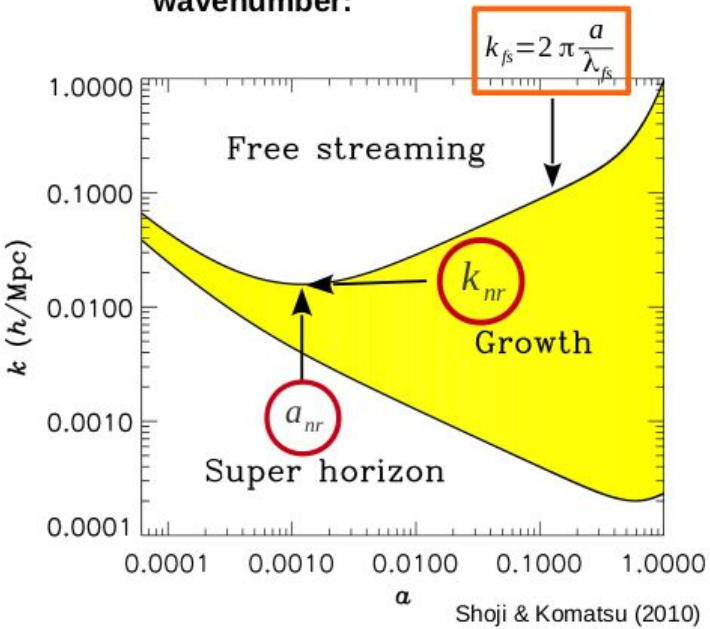

Shoji & Komatsu (2010)

THE HALO MASS FUNCTION: MASSIVE NEUTRINOS

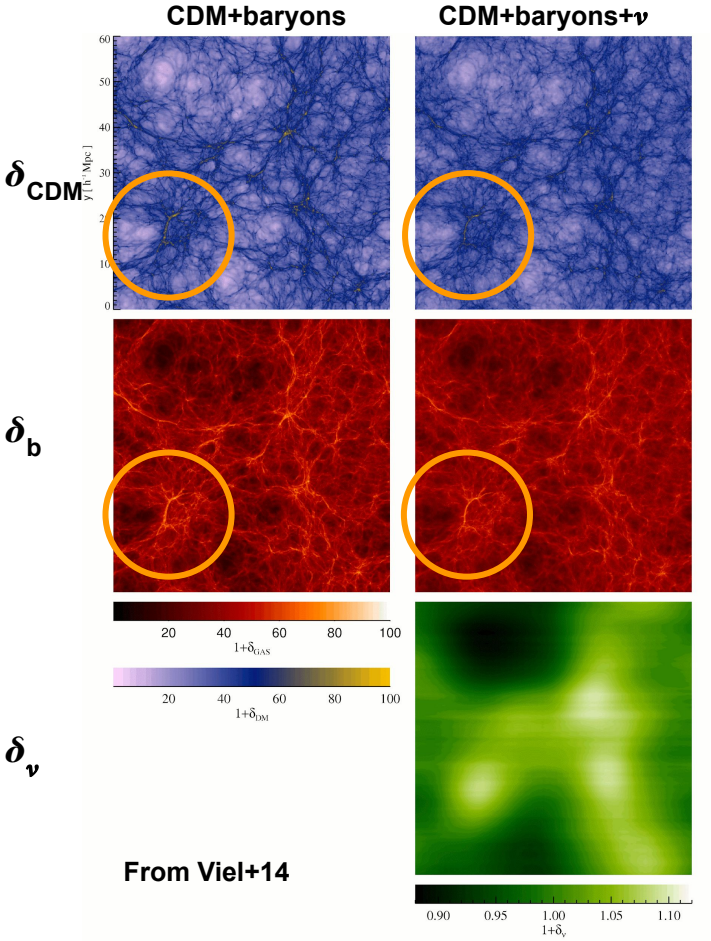

Massive neutrinos:

- Delay the epoch of matter-radiation equality
- Suppress the growth of density fluctuation on scale smaller than the free-streaming length

Effects on the number density of halos as a function of mass

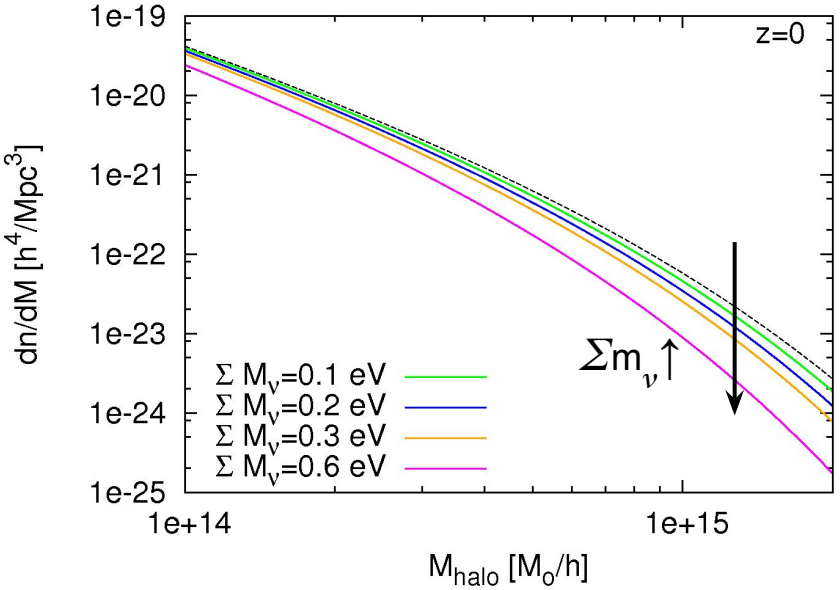

THE HALO MASS FUNCTION: MODIFIED GRAVITY

Modified gravity models, e.g. *f*(R):

$$S = \frac{1}{16\pi G}\int \sqrt{-g}[R + f(R)]d^4x$$

- Give rise to accelerated expansion and enhance gravity
- Introduce screening mechanism that restores GR in high density environments

Relative effect on the Halo Mass Function compared to ΛCDM

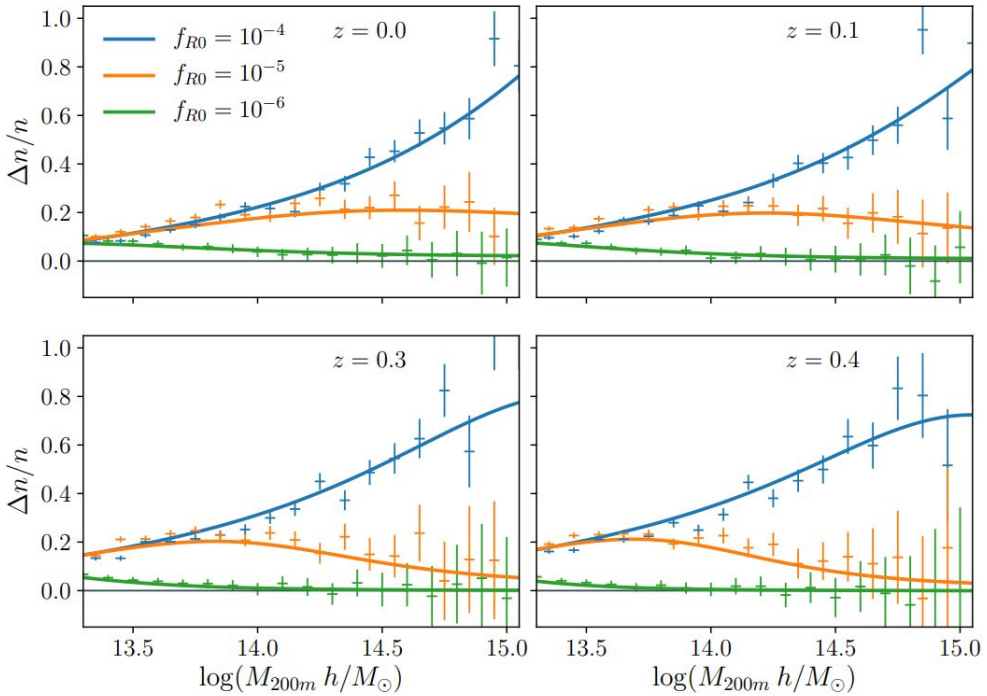

From Hagstotz+18

THE MULTIPLICITY FUNCTION: $f(\sigma)$

Halo mass function: $n(z,M)=\frac{\rho_m}{M} f(\sigma) \frac{d\ln(\sigma^{-1})}{dM}$

- **$f(\sigma)$ "universal" function:**
  - **Press & Schechter (1974) approximated from spherical collapse of Gaussian density field**
  - **Improved modeling using ellipsoidal collapse, e.g. Sheth & Tormen (1999)**
  - **Nowadays calibrated against N-body simulations**

Reference	Functional form
Press & Schechter (1974)	$f_{\rm PS}(\sigma) = \sqrt{\frac{2}{\pi}}\ \frac{\delta_c}{\sigma}\ \exp\left(-\frac{\delta_c^2}{2\sigma^2}\right)$
Sheth & Tormen (1999)	$f_{\rm ST}(\sigma) = A\sqrt{\frac{2a}{\pi}}\ \frac{\delta_c}{\sigma} \exp\left(-\frac{a\ \delta_c^2}{2\sigma^2}\right)\ \left[1+\left(\frac{\sigma^2}{a\ \delta_c^2}\right)^p\right]$
Jenkins et al. (2001)	$f_{\rm J}(\sigma) = A\exp\left(-\lvert\ln\sigma^{-1}+{\rm B}\rvert^{\rm P}\right)$
Reed et al. (2003)	$f_{\rm R}(\sigma) = f_{\rm ST}(\sigma)\exp\left(\frac{-a}{\sigma(\cosh 2\sigma)^b}\right)$
Warren et al. (2006)	$f_{\rm W}(\sigma) = A\left(\sigma^{-a}+b\right)\exp\left(-\frac{c}{\sigma^2}\right)$
Tinker et al. (2008)	$f_{\rm T}(\sigma) = A\left[\left(\frac{\sigma}{b}\right)^{-a}+1\right]\exp\left(-\frac{c}{\sigma^2}\right)$

Pillepich+10

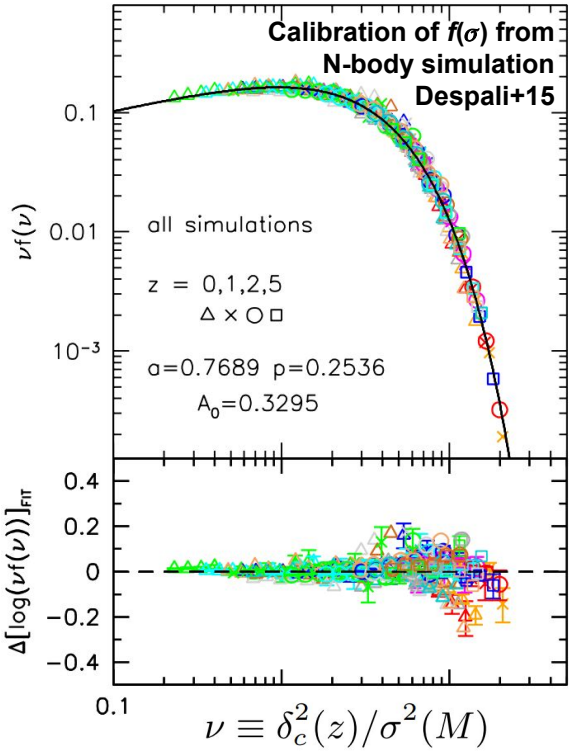

See also: Despali+15 ; Castro+22

HALO MASS FUNCTION: UNIVERSALITY

How accurate is the calibration of f(σ)? Is it universal?

- **Specific of the simulation (e.g. box size, number of particles, softening length)**
- **Halo finder (e.g. linking length, FoF, SO)**
- **Mass definition (e.g. $M_{200,m}$, $M_{500,c}$)**
- **Redshift dependence**
- **Cosmological model (e.g. LCDM, wCDM, massive neutrino)**

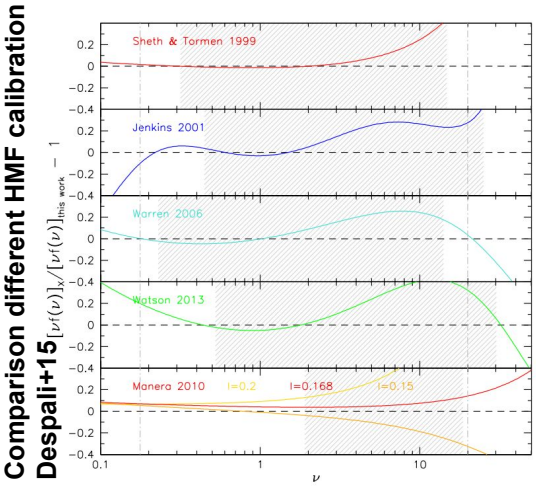

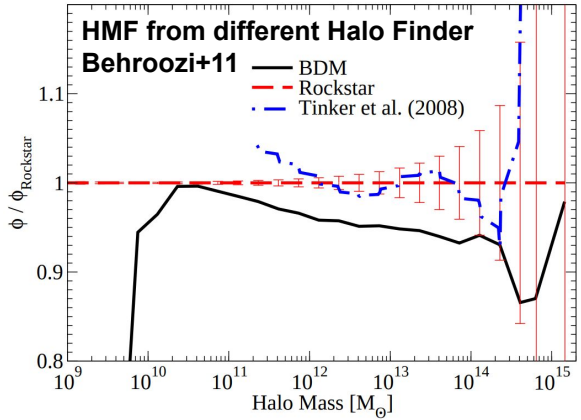

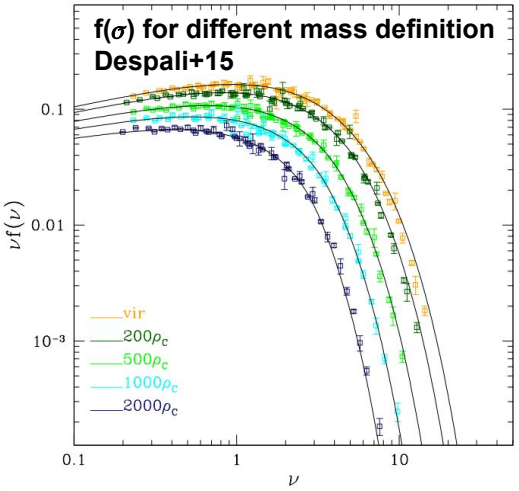

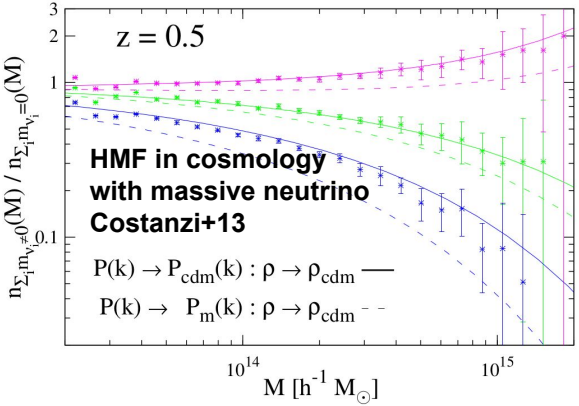

HALO MASS FUNCTION: BARYONIC EFFECTS

Baryonic feedbacks (radiative cooling, star formation, AGN feedback) redistribute and expel mass from galaxy clusters

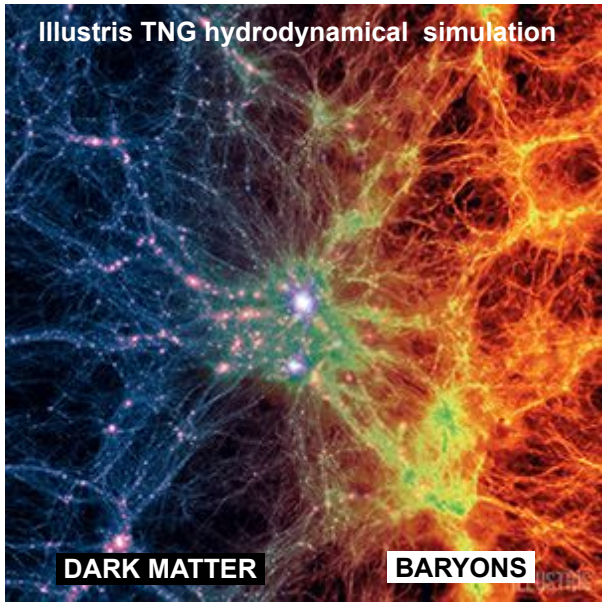

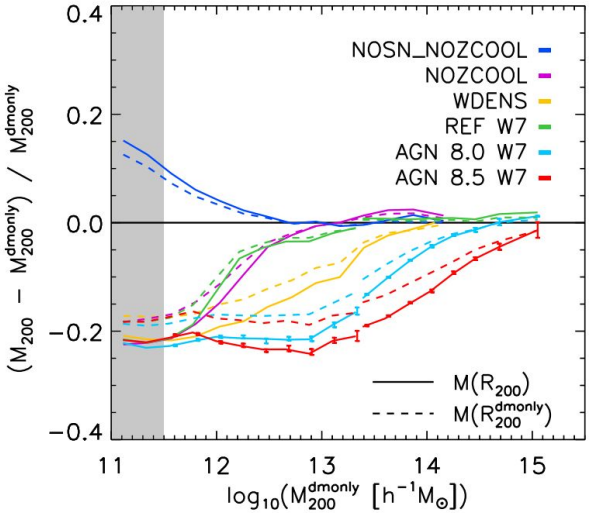

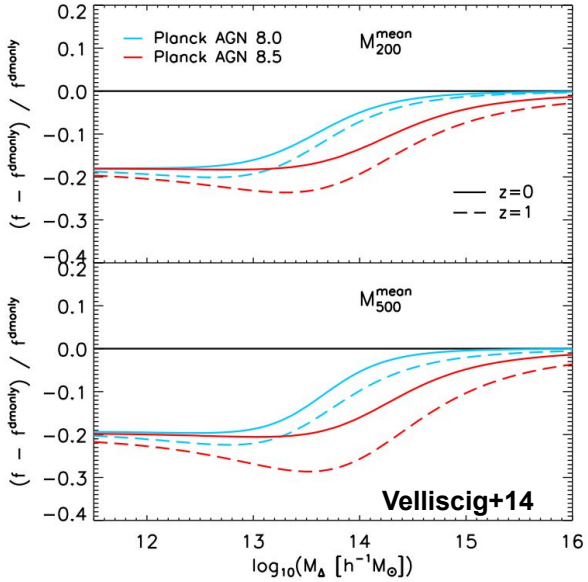

Baryonic feedbacks most effective in the inner the regions of the halo and in low mass systems

See also Castro+21

FROM THEORY TO OBSERVATION

- **Masses are not directly observable. Galaxy clusters are selected according to some observable, in general related to the observational technique, which correlate with the mass.**

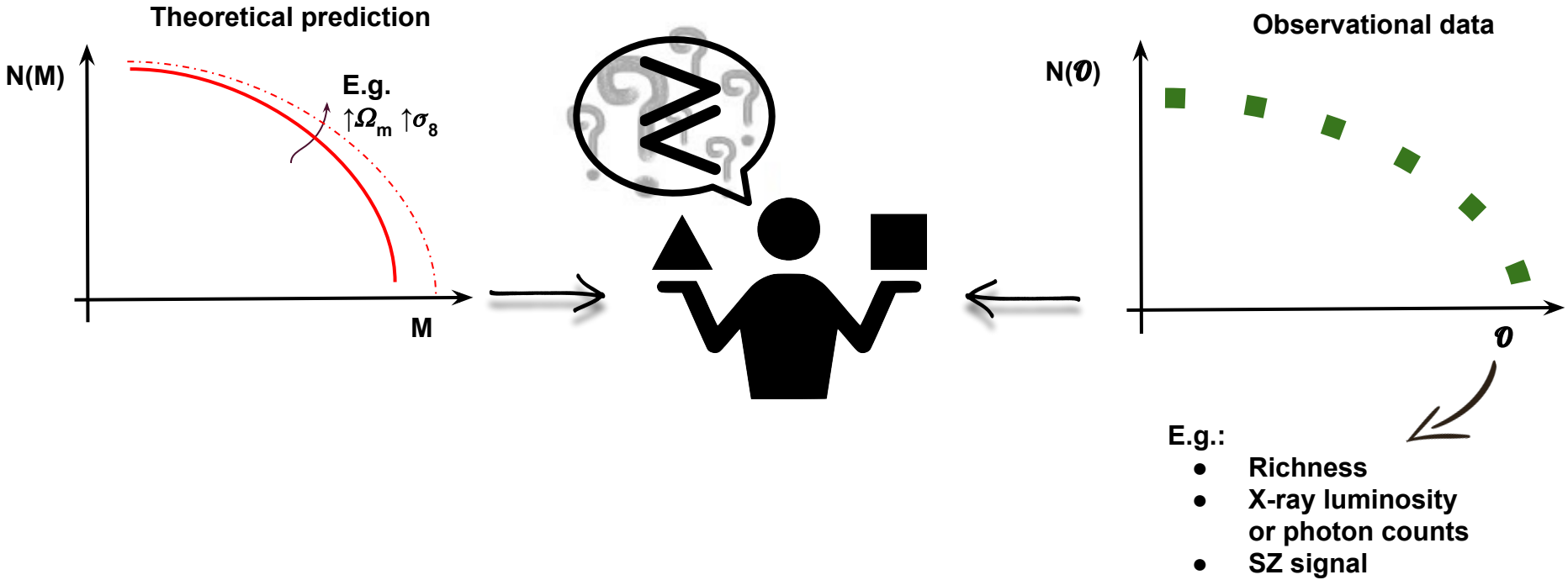

FROM THEORY TO OBSERVATION

- Individual mass measurements are expensive and not feasible for cluster survey. We need to rely on mass proxies which are tightly correlated with the halo mass.

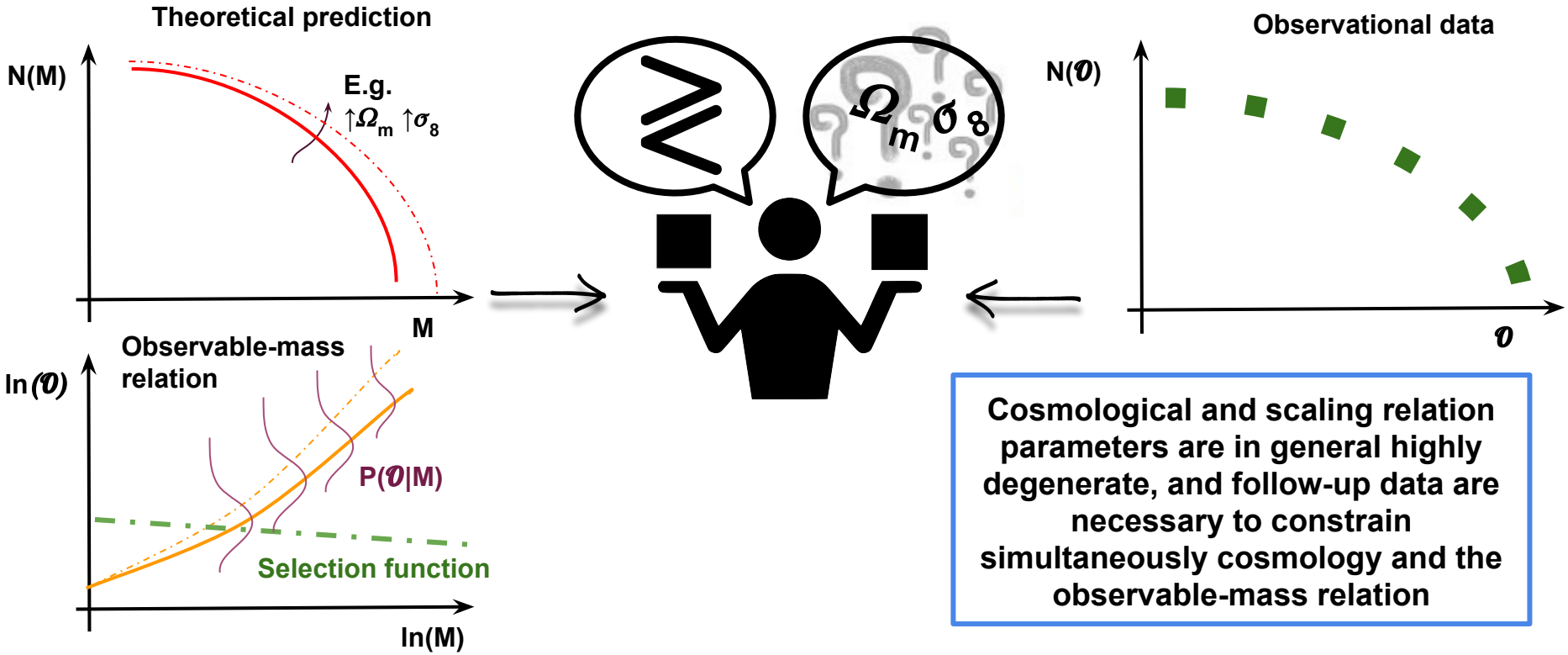

Cosmological and scaling relation parameters are in general highly degenerate, and follow-up data are necessary to constrain simultaneously cosmology and the observable-mass relation

FROM THEORY TO OBSERVATION: CONSTRAINTS

- Combine cluster abundance and cluster mass estimates data to **simultaneously** constrain cosmology and the observable-mass relation(s)

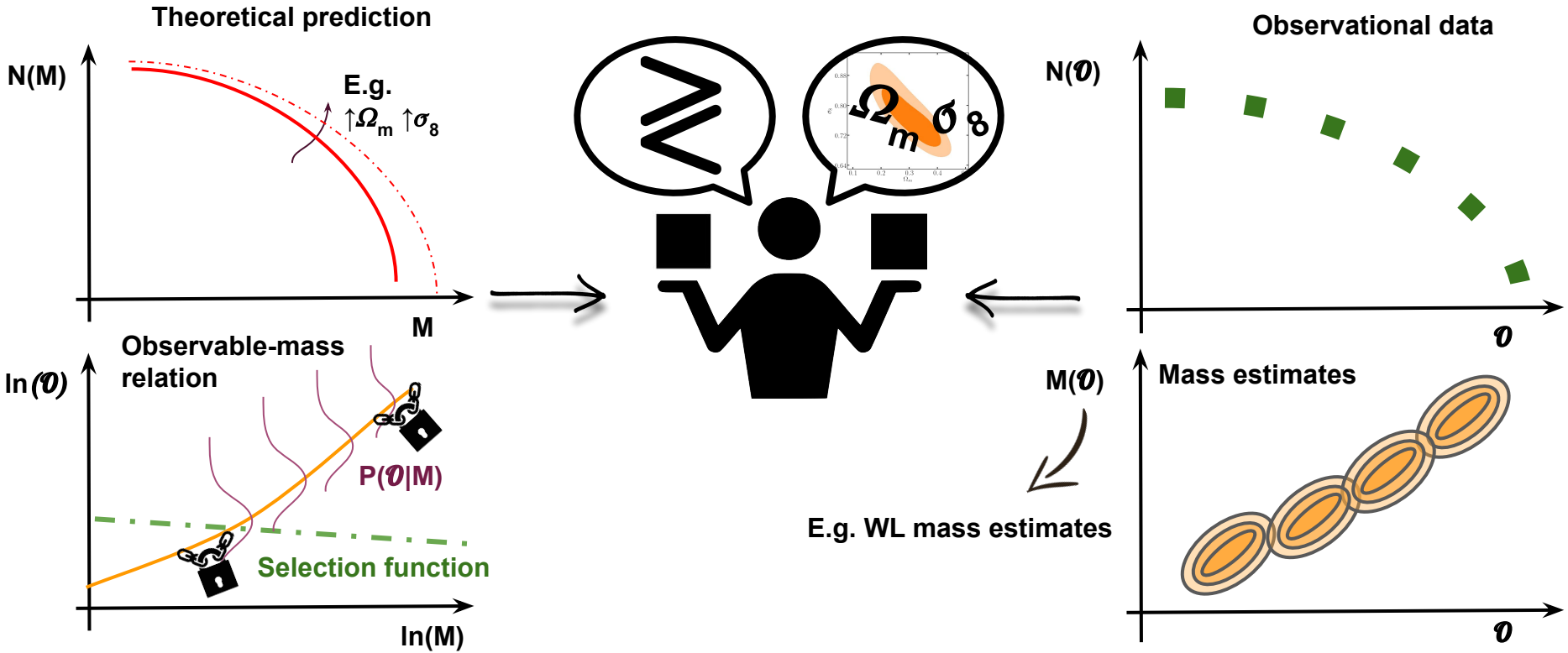

LIMITATIONS FOR CLUSTER COSMOLOGY STUDIES

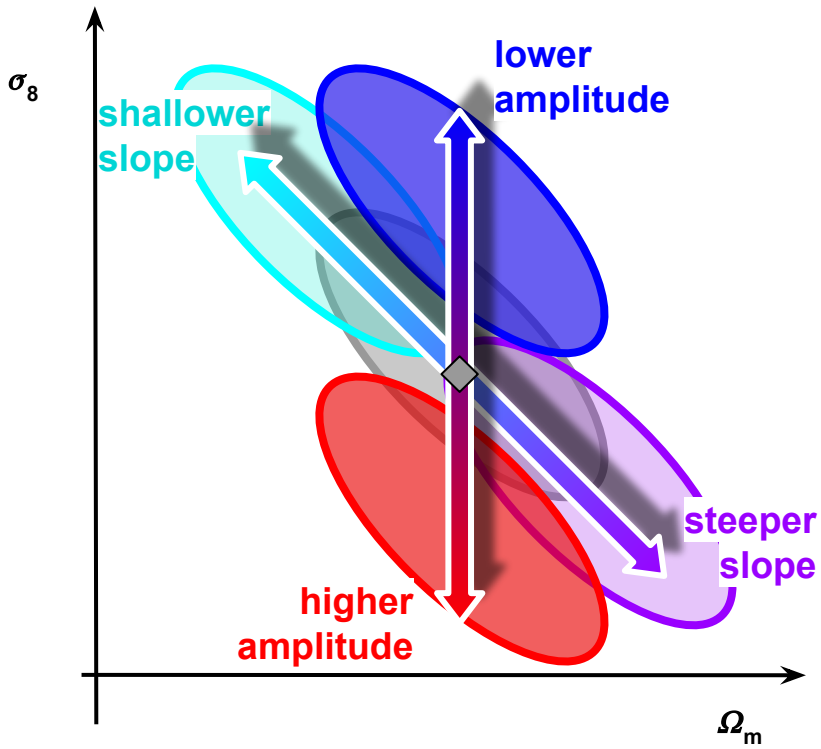

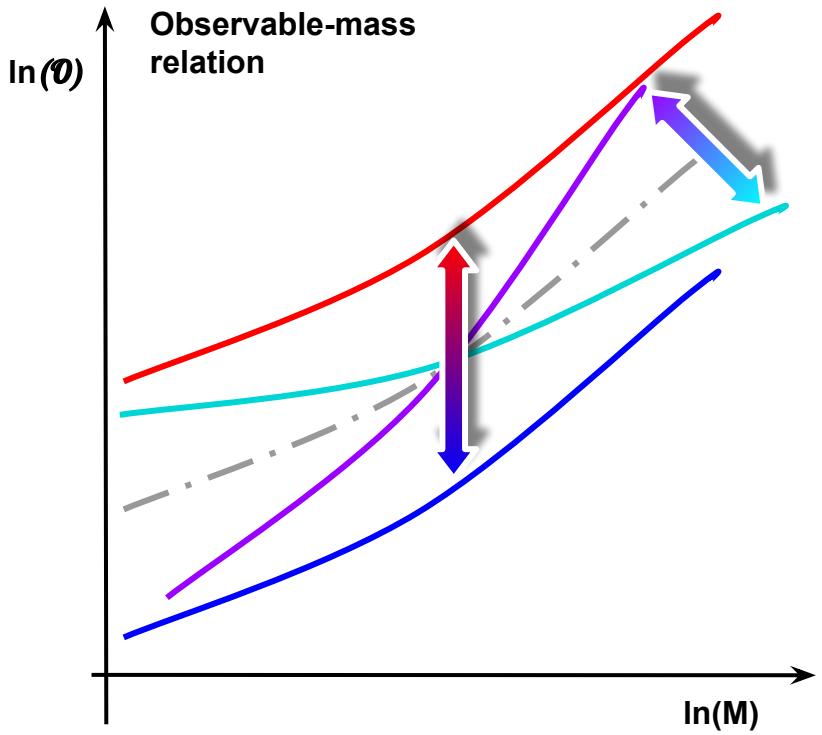

CLUSTER DETECTION: PHOTOMETRIC SURVEY

- **Detection:**
  - **Overdensity of (red-sequence) galaxies**
  - **Lensing effect**

- **Observable/Mass proxy:**
  - **Richness (# member galaxies)**
  - **Luminosity**
  - **Lensing signal**
  - **Velocity dispersion (with spectra)**

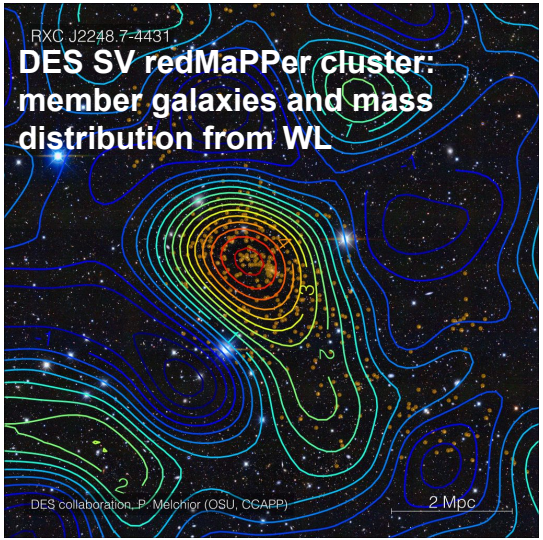

***z*-λ distribution of redMaPPer clusters in DES Y1**

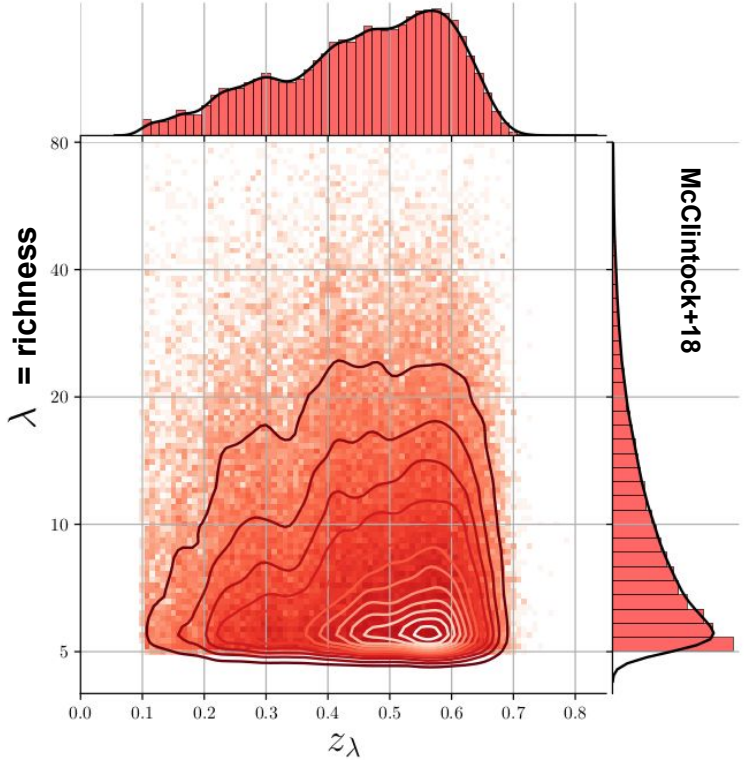

CLUSTER DETECTION: X-RAY SURVEY

- **Detection:**
  - **Extended x-ray sources**

- **Observable/Mass proxy:**
  - **L_X**
  - **T_X**
  - **Flux**
  - **$Y_X = M_{gas}\ T_X$ (gas thermal energy)**

X-ray images of clusters from eROSITA

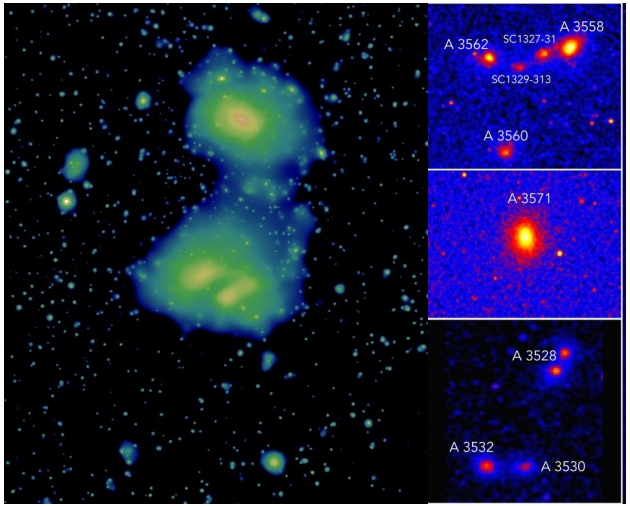

L_X, z distribution of X-ray selected catalogs

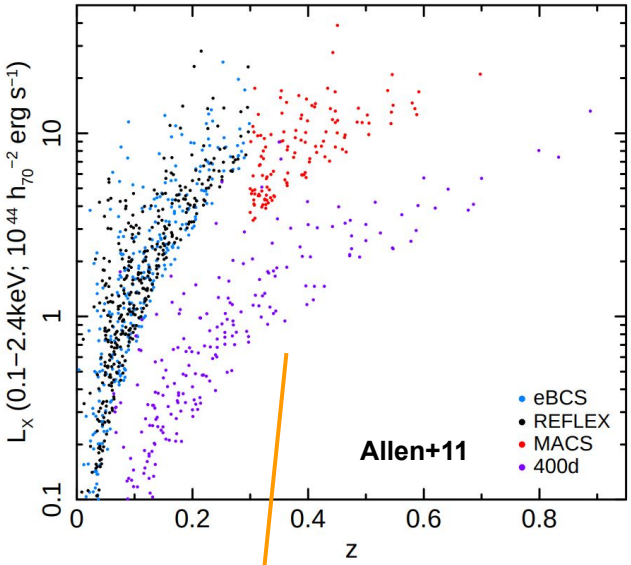

Flux limited sample

- **X-ray emissivity from *bremsstrahlung* radiation of the ICM:**

$$\epsilon_\nu \equiv \frac{\mathrm{d}L}{\mathrm{d}V\mathrm{d}\nu} \propto n_e^2 g(\nu, T) T^{-1/2} \exp(-h\nu/k_B T)$$

Not very sensitive to projections

CLUSTER DETECTION: SZ SURVEY

- **Detection:**
  Thermal Sunyaev-Zel'dovich effect (mm-wavelength)

- **Observable/Mass proxy:**
  SZ signal

Thermal Sunyaev-Zel'dovich effect

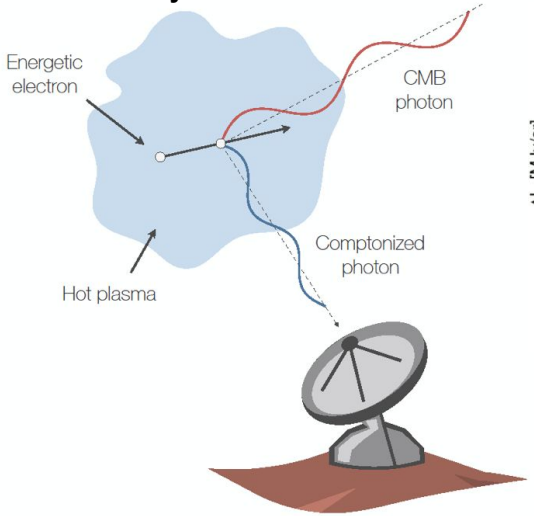

SZ spectral distortion

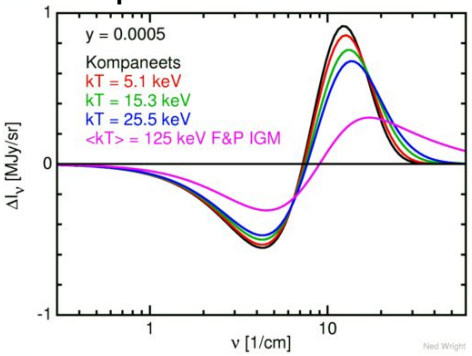

Compton-y parameter

$$y = \int \mathrm{d}l \frac{k_B T_e}{m_e c^2} n_e \sigma_T$$

Mass and redshift distribution of SZ-selected cluster catalogs (Bleem+19)

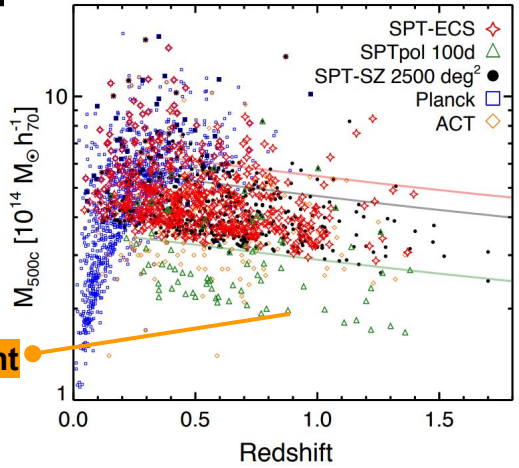

~ redshift independent

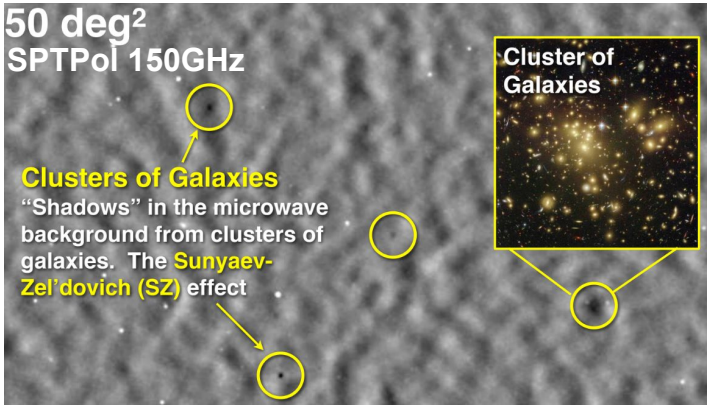

Credits B. Benson, SPT Collaboration

CLUSTER CATALOGS AT DIFFERENT λs

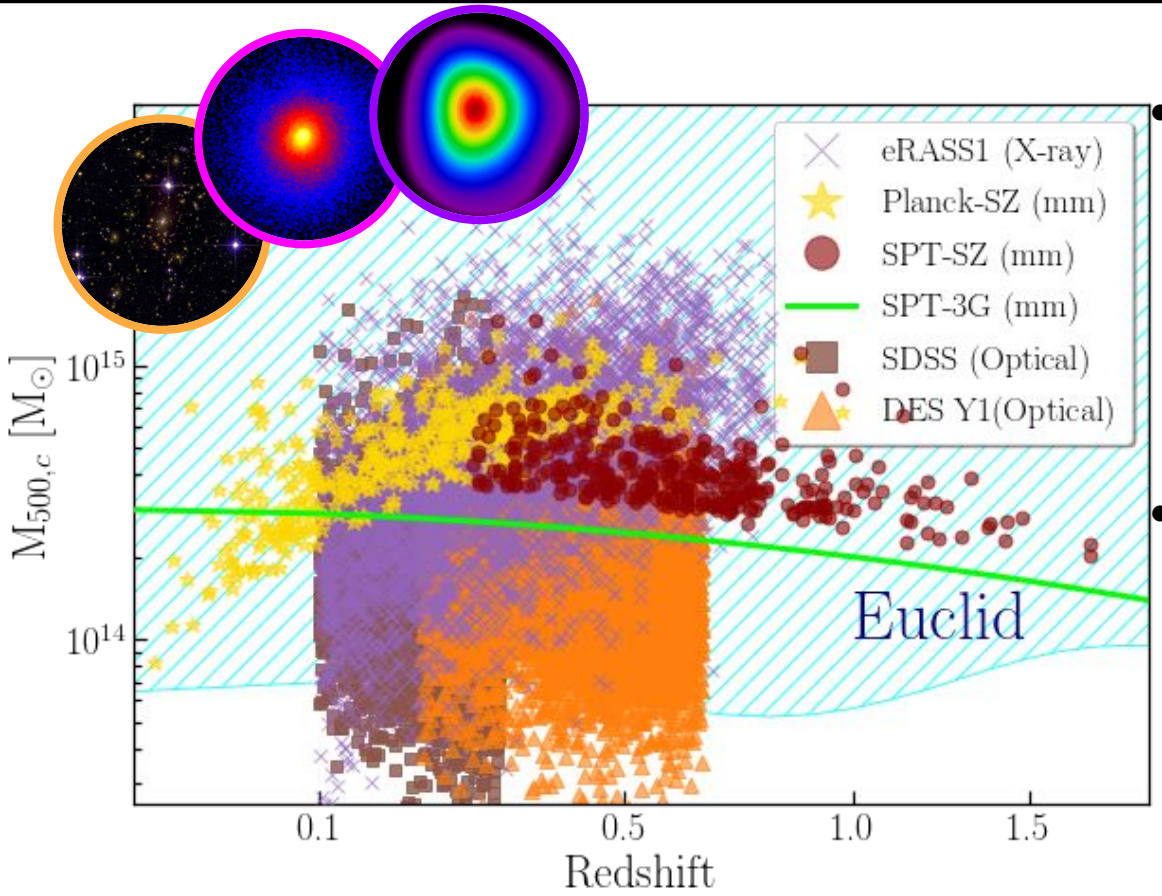

- **ICM-selected (X-ray, SZ):**
  - **Mass limit M~2 · 10^{14} $M_\odot$**
  - **Clean selection function (SZ signal independent of redshift!)** 👍
  - **Need optical follow-up for confirmation, redshift and WL data** 👎
- **Optically-selected:**
  - **Lower mass limit M~5 · 10^{13} $M_\odot$ (x10 sample size)** 👍
  - **Selection function harder to model** 👎
  - **WL and photo-z data readily available** 👍

MASS MEASUREMENTS FROM X-ray DATA

- **From hydrostatic equilibrium:**

$$M(<r) = -\frac{r}{G}\frac{k_B T(r)}{\mu m_p}\left(\frac{\mathrm{d}\ln\rho_{\mathrm{gas}}(r)}{\mathrm{d}\ln r} + \frac{\mathrm{d}\ln T(r)}{\mathrm{d}\ln r}\right)$$

Assumptions:

- **Hydrostatic equilibrium (Negligible non-thermal pressure support)**
- **Spherical symmetry**

For dynamically relaxed cluster: $M_{HE} / M_{true} \sim 0.85$ $\sigma_{M\_HE} \sim 10\%$

Temperature profiles from *XMM-Newton* observations (Pratt+06)

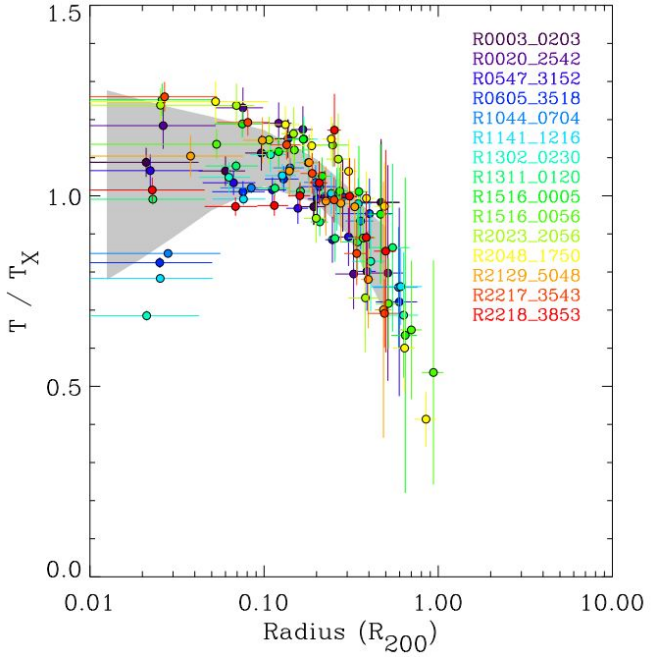

MASS MEASUREMENTS FROM SPECTROSCOPIC DATA

- **Dynamical mass estimates (Jeans equation):**

$$M(<r) = -\frac{r\sigma_r^2}{G}\left(\frac{\mathrm{d}\ln\sigma_r^2}{\mathrm{d}\ln r} + \frac{\mathrm{d}\ln n_{\mathrm{glx}}}{\mathrm{d}\ln r} + 2\beta\right)$$

Radial velocity dispersion — Velocity anisotropy parameter

Assumptions:
- **Spherical symmetry**
- **Dynamical equilibrium**

- **Caustic method (projected phase-space distribution):**

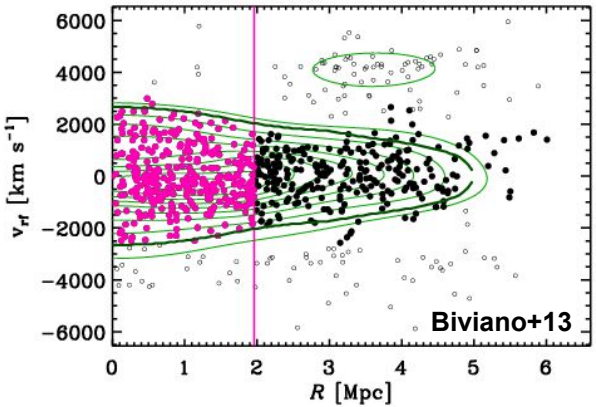

L.o.s. velocity dispersion and member galaxy density profiles from VLT/VIMOS (Biviano+13)

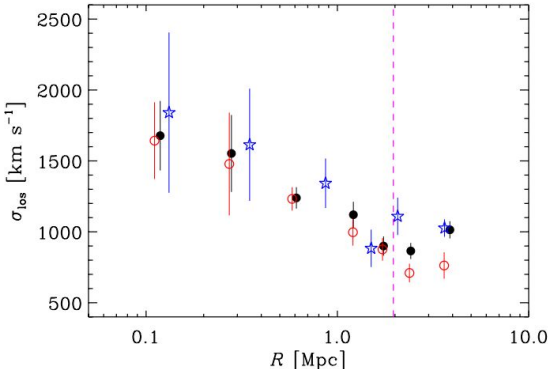

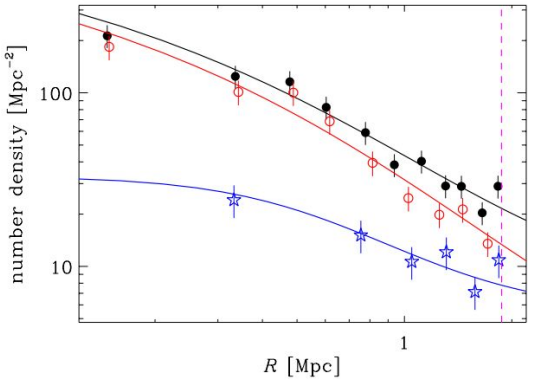

MASS MEASUREMENTS FROM SPECTROSCOPIC DATA

- **Dynamical mass measurements in Euclid:**

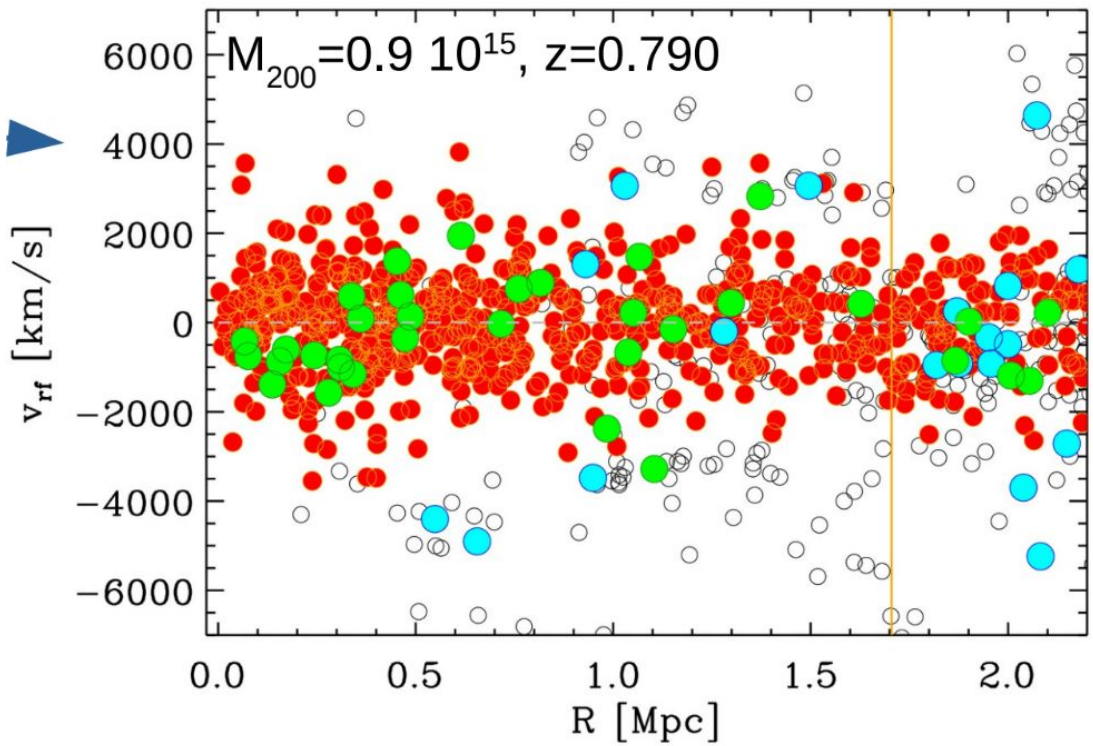

Credit A. Biviano

MASS MEASUREMENTS FROM IMAGING

Strong Lensing mass measurements:

- **Strong lensing regime in cluster's core (~few hundred kpc)**
- **Deflection of the light is large enough to create multiple images of the same source and arcs → Precise measurements of the projected mass in scales enclosed by arcs**
- **The mass reconstruction rely on assumptions on lens geometry and mass model → introduce systematic uncertainties of ~10–20%**

Projected density profile from strong lensing

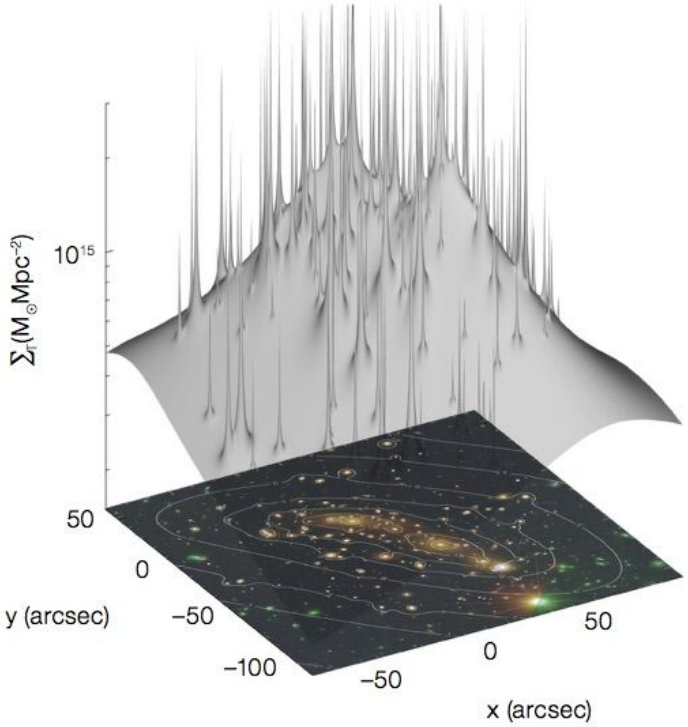

MASS MEASUREMENTS FROM IMAGING

Weak Lensing mass measurements:

- At larger radii (R > 300 kpc), the tidal gravitational field causes subtle distortion of the shape of background galaxies – weak lensing regime – resulting in a coherent alignment of the sources
- we can reconstruct the projected density profile by measuring the mean tangential shear profile at different radii around the cluster

$$\gamma_t(n_s(z), \Sigma(R)) \Rightarrow \Sigma(R) = \int_{-\infty}^{\infty} d\chi \, \Delta\rho\left(\sqrt{R^2 + \chi^2}\right)$$

- To infer the mass profile one need to assume a parametric form for the halo density profile **e.g. NFW, Einasto profiles; Navarro+97, Einasto 1965) and correlated structures (2-halo term)**
- In wide-field surveys, the weak lensing signal of clusters is usually stacked to increase the signal-to-noise and reduce the effect of **shape noise** and **projection systematics**, enabling calibration of the **mass–observable scaling relation** across large cluster samples.

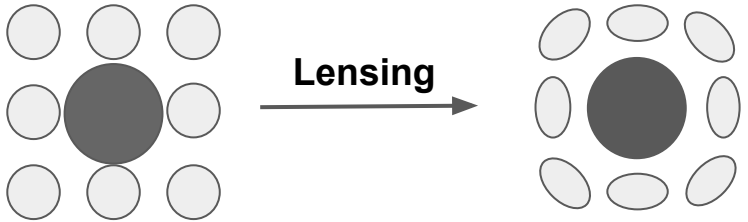

Tangential shear profile from WL (Dietrich+18)

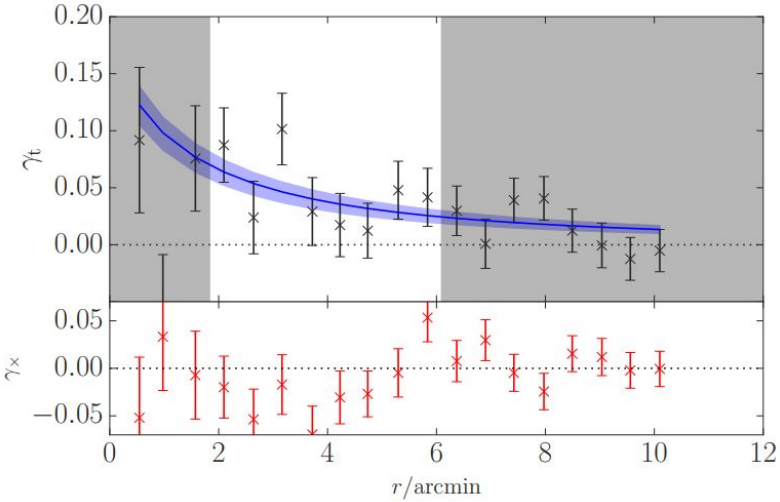

MASS MEASUREMENTS FROM IMAGING

Cluster mass profile from different techniques (Battaglia+16)

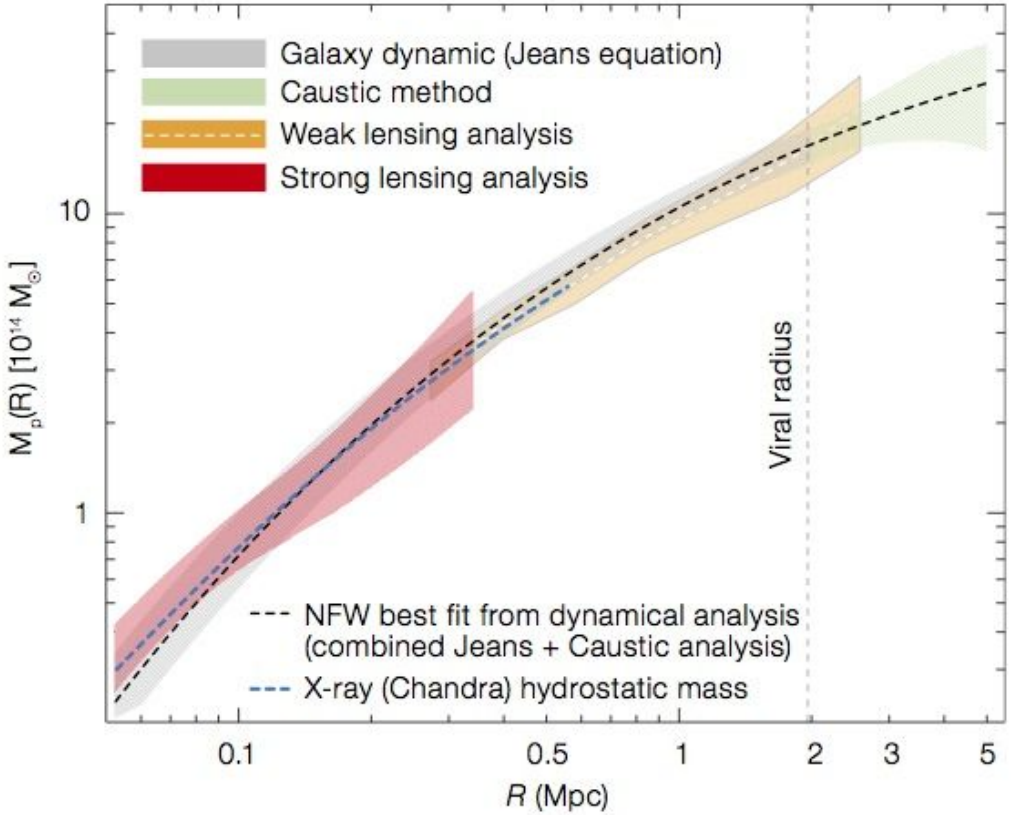

CMB CLUSTER LENSING

- **Lensing by GC induces a dipole-like distortion in the CMB:**

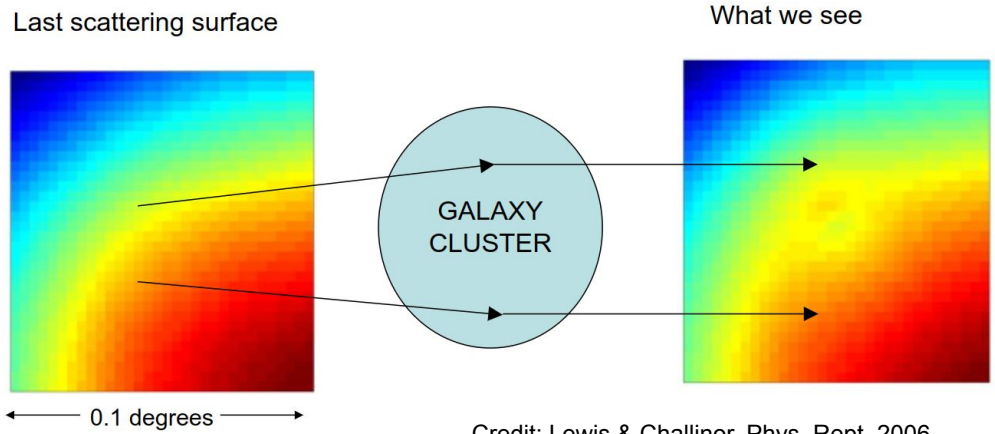

Credit: Lewis & Challinor, Phys. Rept. 2006

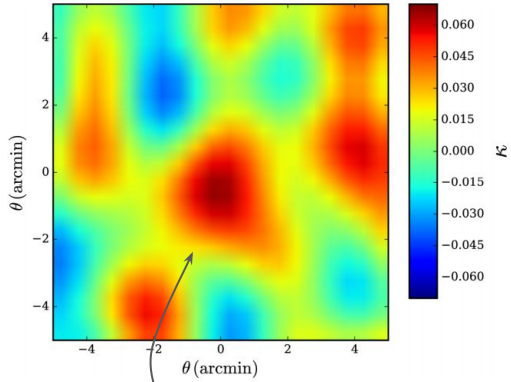

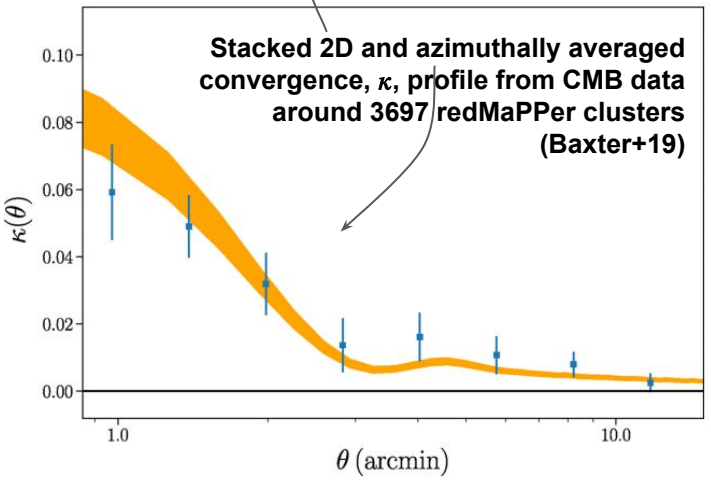

The distortion is quite small (~10μK for $10^{15}M_{\odot}$ halo) but can be used to calibrate the mass of high redshift clusters.

CMB CLUSTER LENSING

CMB lensing signal can also be detected in polarization data:

- **CMB Polarization (E-modes) provides a "cleaner" signal than temperature → Less contaminated by astrophysical foregrounds (e.g., tSZ effect, point sources)**

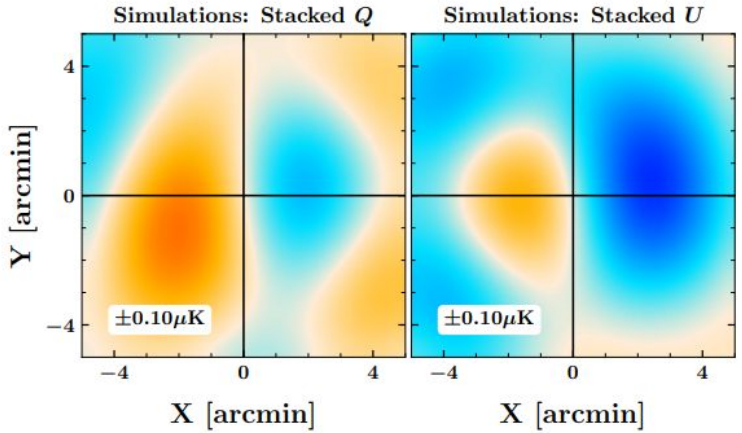

FIG. 1. Example lensing dipole signal extracted from low-noise simulated Q/U stacks. The stack includes contributions from 10,000 clusters. The background, estimated from random locations, has been subtracted to remove the large-scale CMB gradient signals from both the panels.

4.8 σ detection of lensing signal from SPT-Pol data alone (Raghunathan+19)

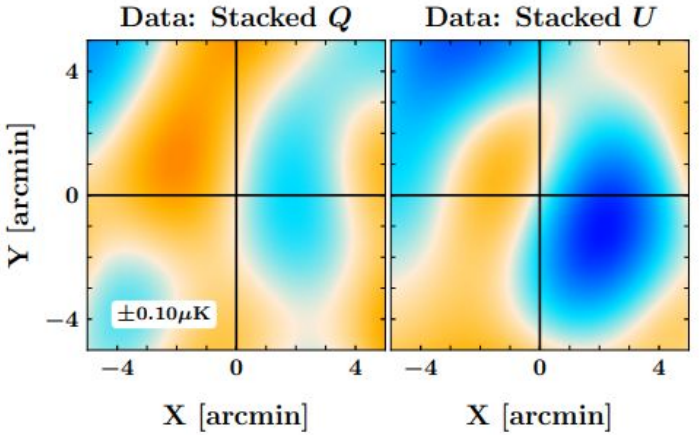

FIG. 3. Rotated, background-subtracted Q and U stacks from the SPTpol data showing the cluster lensing dipole signals. Unlike in Fig. 1, these images have been filtered to remove the small-scale noise for illustrative purposes.

FROM THEORY TO OBSERVATION: SCALING RELATIONS

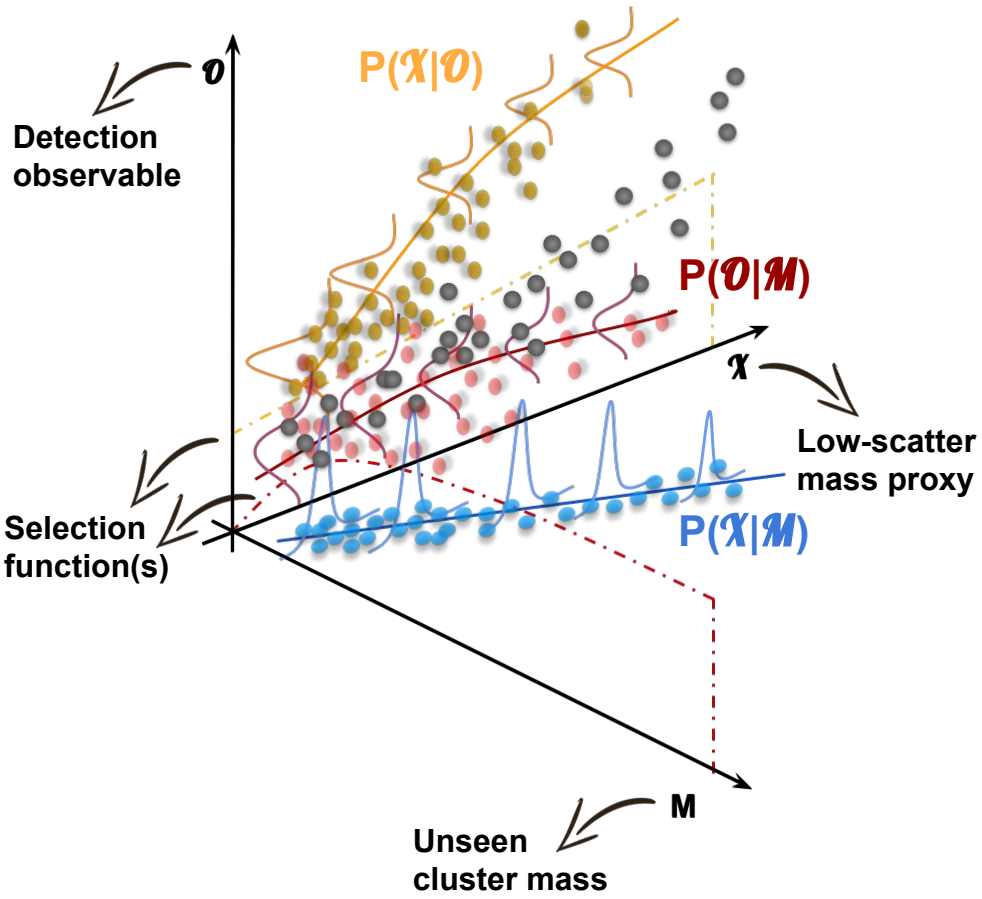

Different detection techniques imply different mass proxies, mass calibration data and systematics.

The calibration of the observable-mass relation(s) requires:

- Well defined selection function(s)
- A model to describe the parent distribution as a function of mass (halo mass function)
- A model to describe the PDF of the multivariate observable space: $P(X,O \mid M)$

FROM THEORY TO OBSERVATION: SCALING RELATIONS

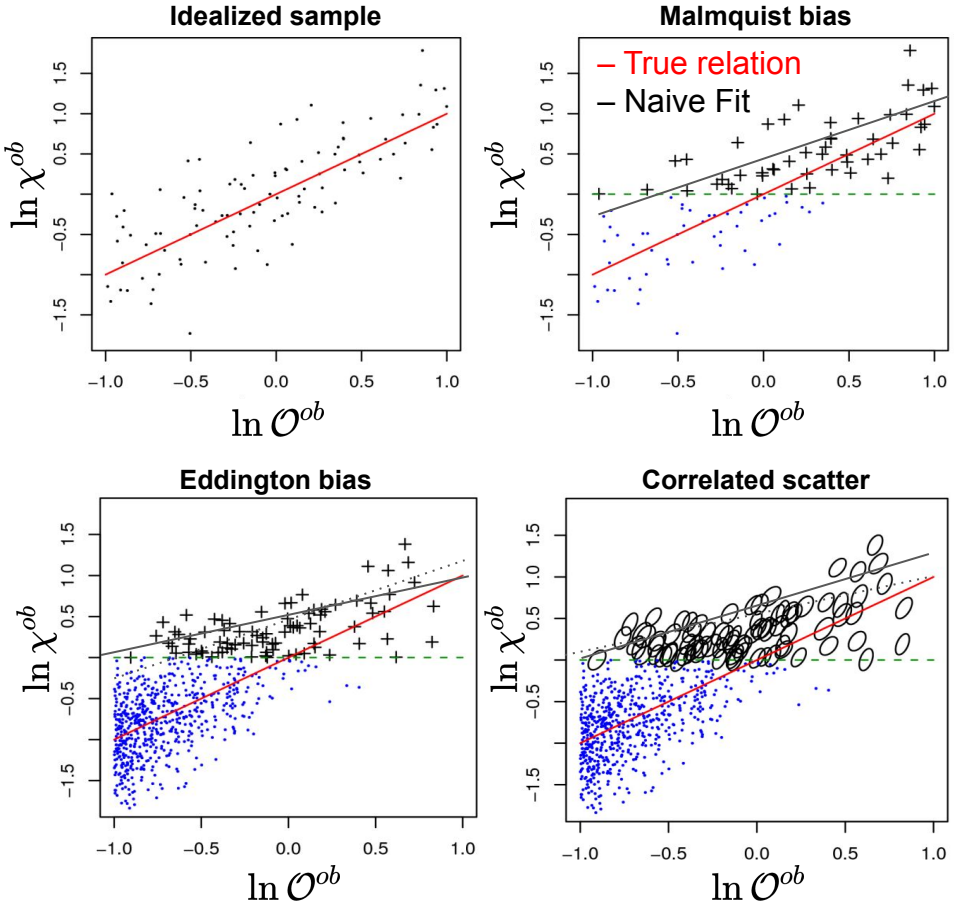

Credit A. Mantz

Different detection techniques imply different mass proxies, mass calibration data and systematics.

The calibration of the observable-mass relation(s) requires:

- **Well defined selection function(s)**
- **A model to describe the parent distribution as a function of mass (halo mass function)**
- **A model to describe the PDF of the multivariate observable space: $P(\mathcal{X},\mathcal{O}|\mathcal{M})$**

CORRELATION BETWEEN MULTI-λ OBSERVABLES

- **Observationally, we only have access to projected quantities.**

Projected cluster mass maps along a cylinder of length 23 Mpc

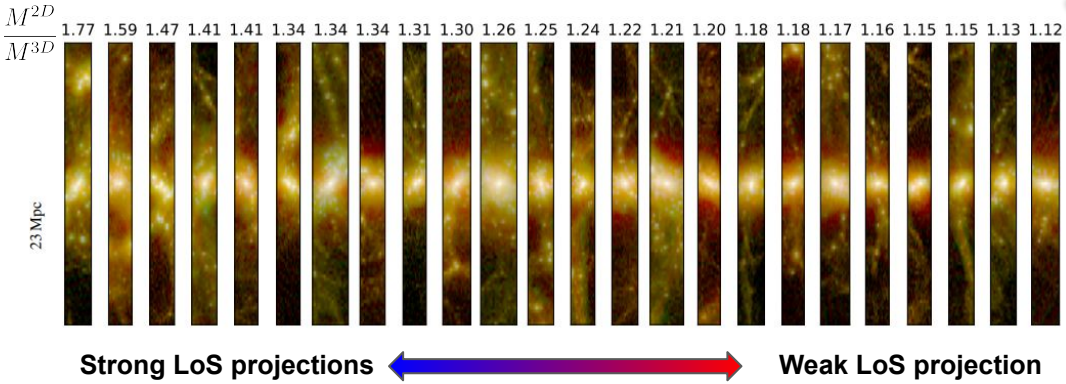

- **Line-of-sigh projections increase the scatter and skewness of the Obs-Mass relations and introduce correlations between observables measured at different wavelengths**

See also e.g. Farahi et al 2019

Correlation coefficients matrix (upper-right triangle) and scatter plot (bottom-left triangle) of log-residual for different 2D observables

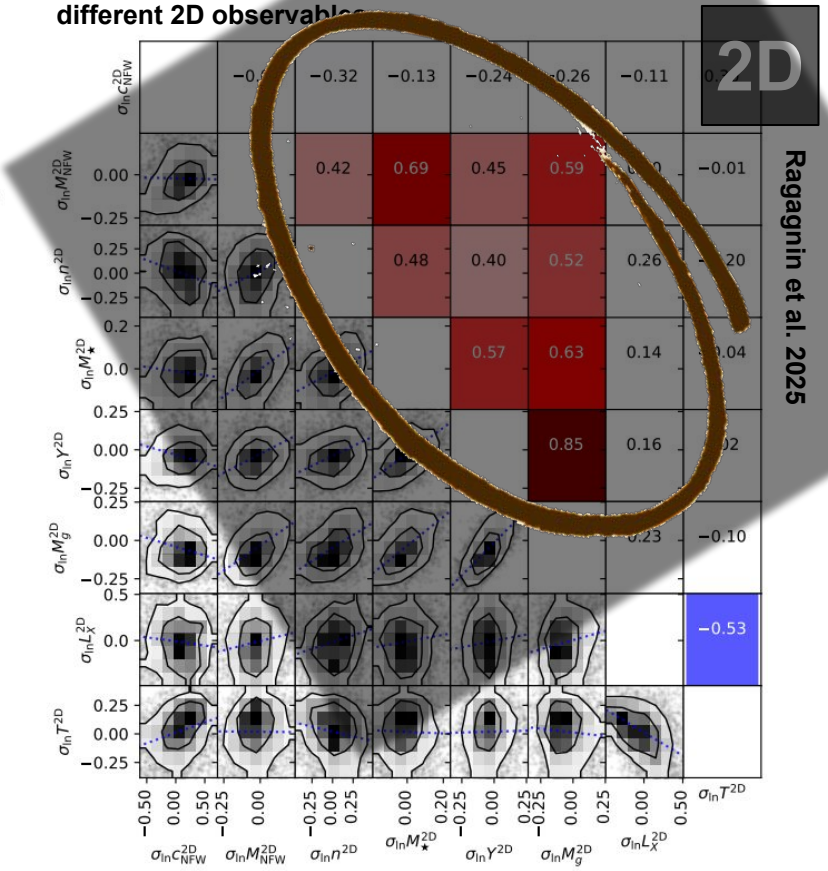

CORRELATION BETWEEN MULTI-λ OBSERVABLES

- **Observationally, we only have access to projected quantities.**

Projected cluster mass maps along a cylinder of length 23 Mpc

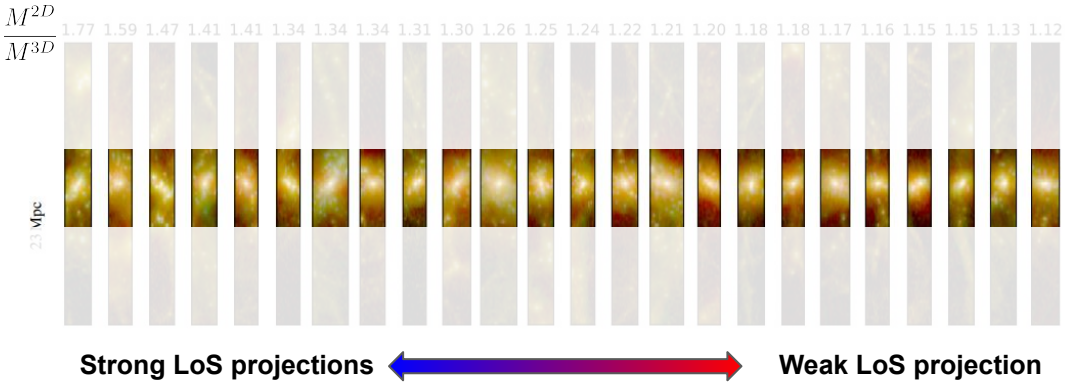

- **Line-of-sigh projections increase the scatter and skewness of the Obs-Mass relations and introduce correlations between observables measured at different wavelengths**

See also e.g. Farahi et al 2019

Correlation coefficients matrix (upper-right triangle) and scatter plot (bottom-left triangle) of log-residual for different 3D observables

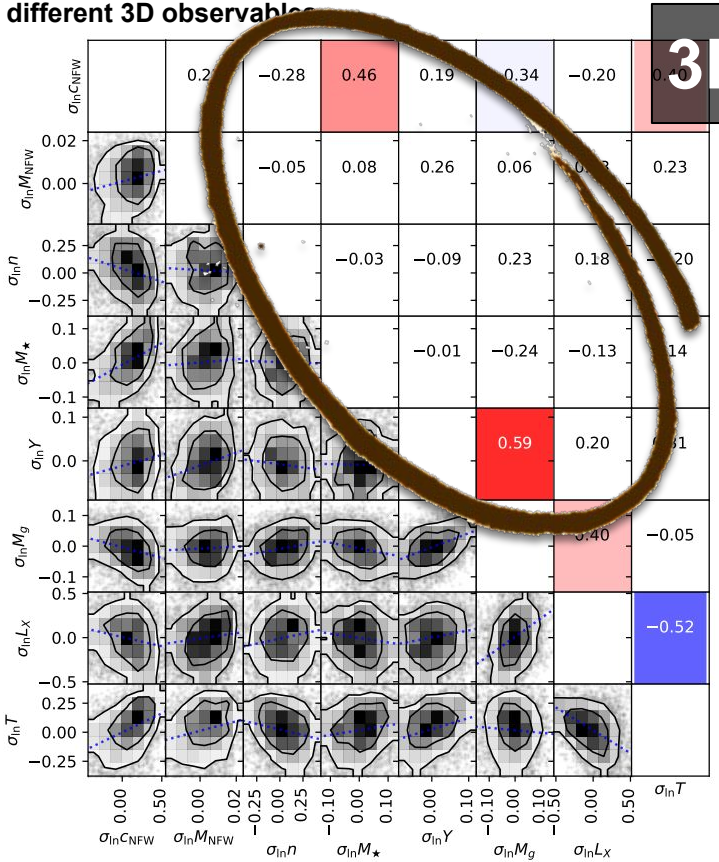

RECENT CONSTRAINTS FROM CLUSTER NC

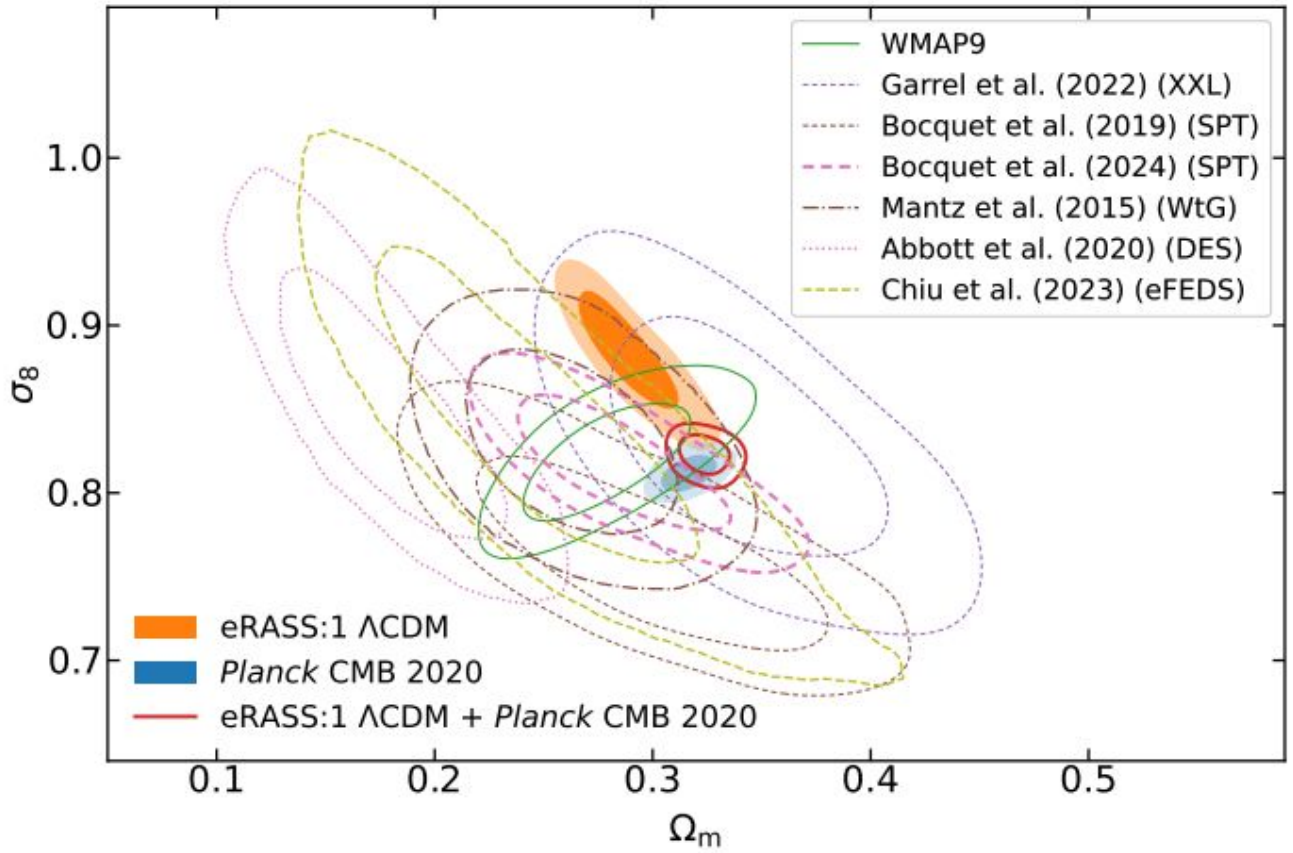

eRASS1:

$$\Omega_m = 0.29^{+0.01}_{-0.02},$$
$$\sigma_8 = 0.88 \pm 0.02,$$
$$S_8 = 0.86 \pm 0.01.$$

https://arxiv.org/pdf/2402.08458.pdf

RECENT CONSTRAINTS FROM CLUSTER NC

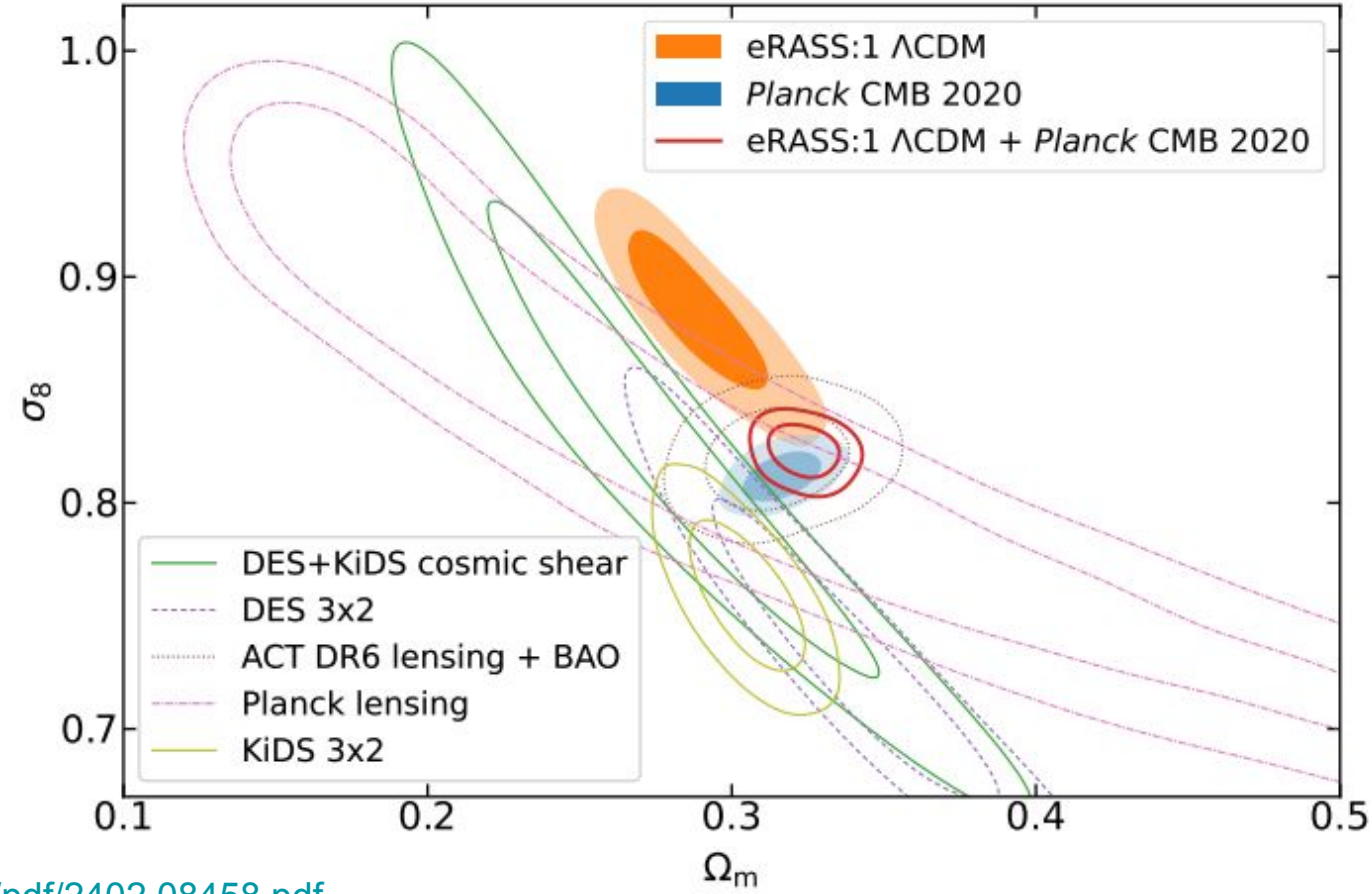

https://arxiv.org/pdf/2402.08458.pdf

RECENT CONSTRAINTS FROM CLUSTER NC

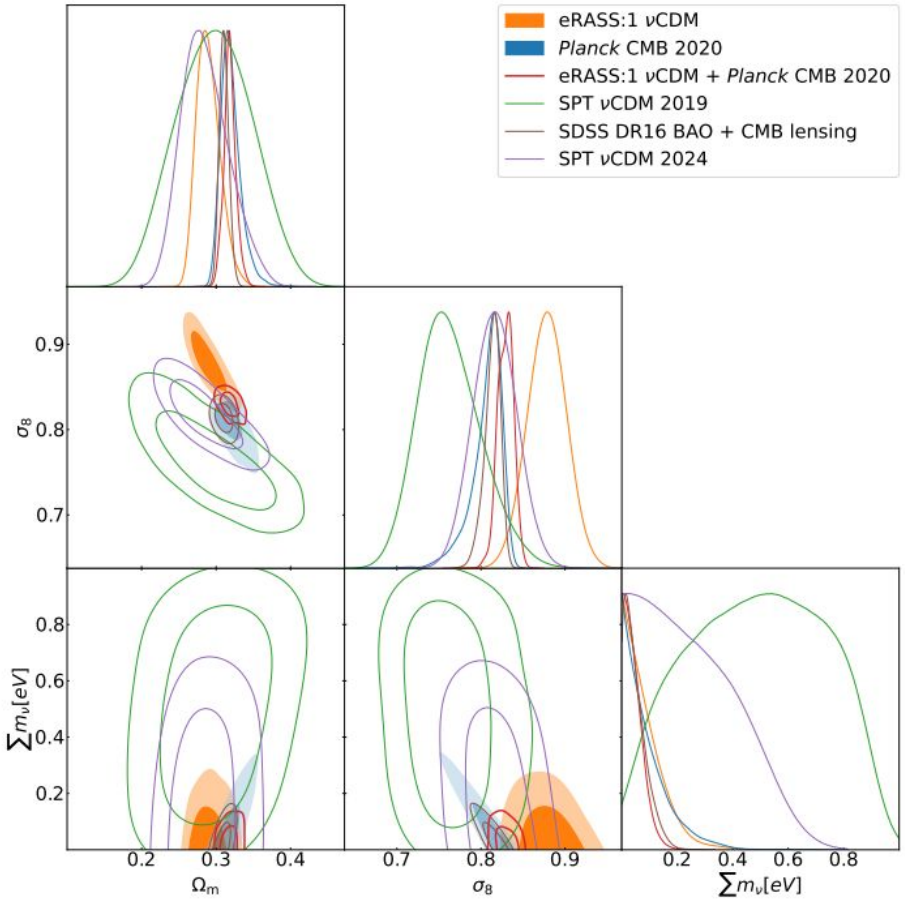

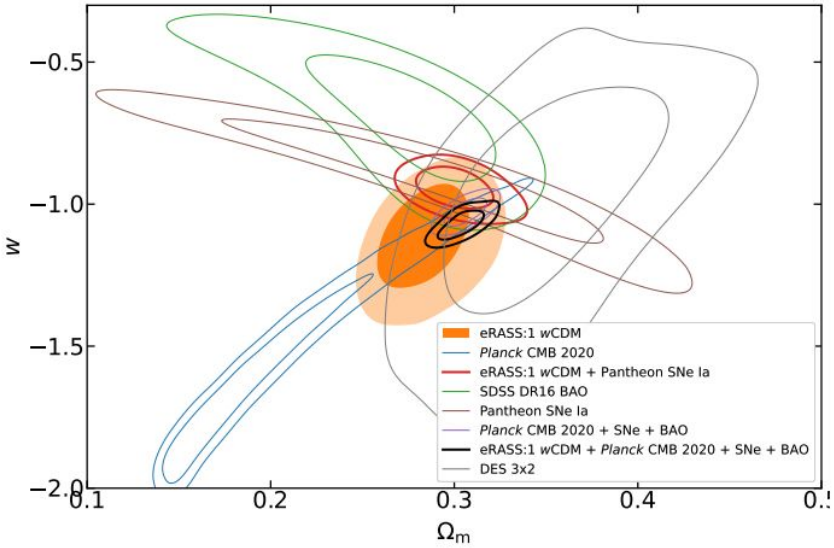

https://arxiv.org/pdf/2402.08458.pdf

LIMITATIONS FOR CLUSTER COSMOLOGY STUDIES

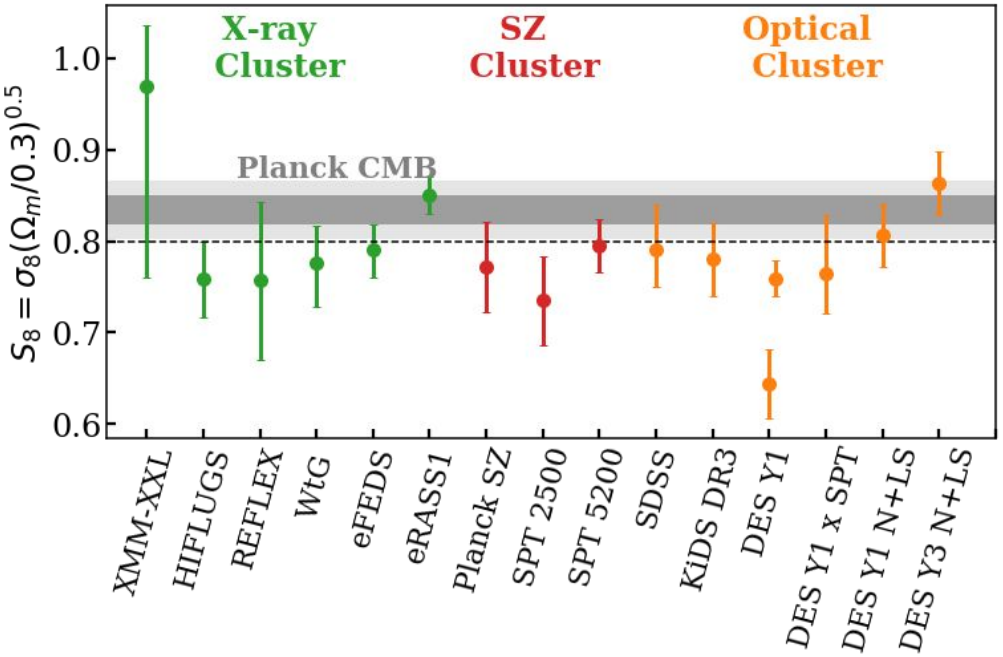

- **Cosmological constraints independent and competitive with other cosmological probes**
- **Slight to moderate tension between different cluster studies**
- **Currently limited by the mass (i.e. scaling relation) calibration**

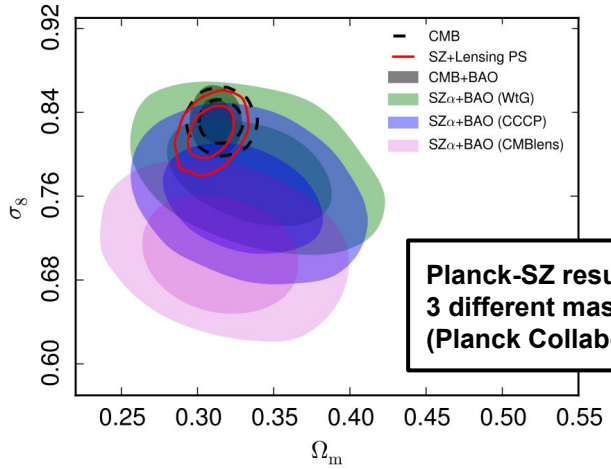

Planck-SZ results assuming 3 different mass calibrations (Planck Collaboration 2015)

OTHER COSMOLOGICAL TESTS WITH GALAXY CLUSTERS

OTHER COSMOLOGICAL TESTS WITH GALAXY CLUSTERS

- **Gas mass fraction (Ω_m,Ω_Λ, w):**

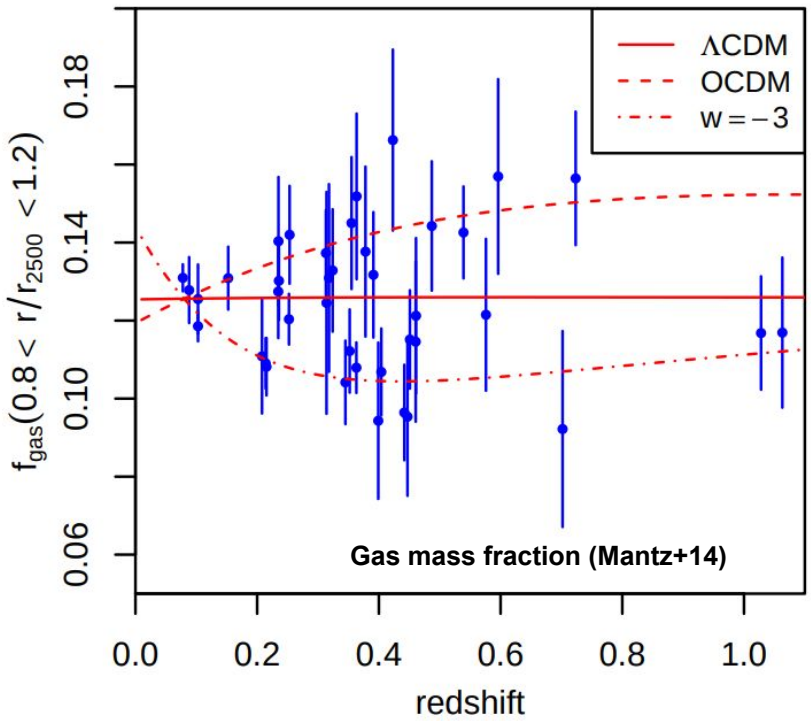

$$f_{\rm gas} = \frac{M_{\rm gas}}{M_{\rm tot}} \propto \left(\frac{\Omega_b}{\Omega_m}\right)\left[\frac{d^{\rm ref}(z)}{d(z)}\right]^{3/2}$$

With priors on

1. $\Omega_{\rm b}h^2$ (important)
2. h (less important),

the low-z data constrain $\Omega_{\rm m}$:

$$f_{\rm gas}(z \lesssim 0.15) \propto \frac{\Omega_{\rm b}}{\Omega_{\rm m}}\, h^{3/2}$$

Apparent evolution constrains dark energy:

$$f_{\rm gas}(z) \propto d(z)^{-3/2}$$

Credit A. Mantz

OTHER COSMOLOGICAL TESTS WITH GALAXY CLUSTERS

- **Gas mass fraction (Ω_m,Ω_Λ, w):**

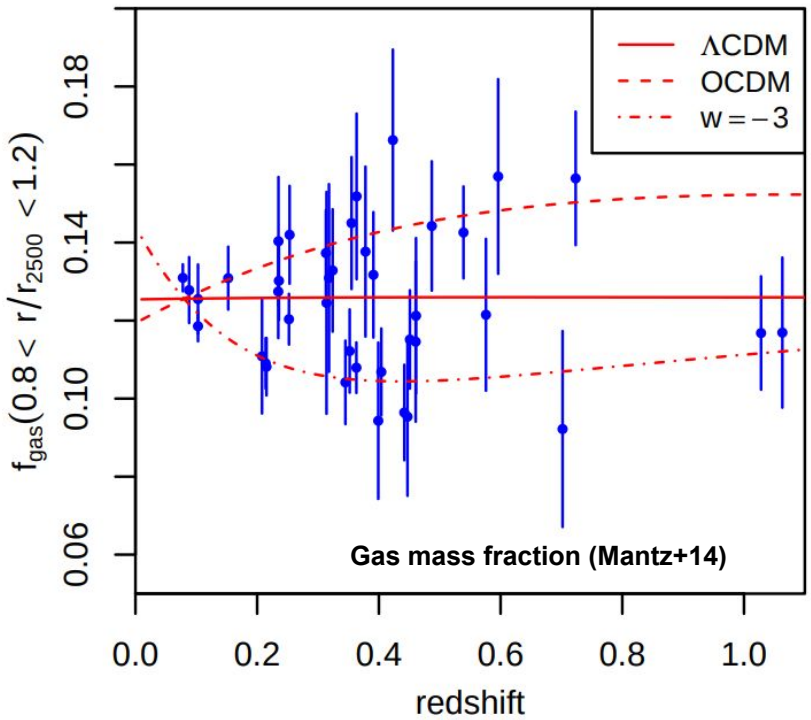

$$f_{\rm gas} = \frac{M_{\rm gas}}{M_{\rm tot}} \propto \left(\frac{\Omega_b}{\Omega_m}\right)\left[\frac{d^{\rm ref}(z)}{d(z)}\right]^{3/2}$$

Main systematics:

- **Uncertainty in the mass estimates (e.g. Hydrostatic bias)**
- **Selection effects → relaxed clusters**
- **f_{gas} changes with radius →Results depends on the chosen aperture for the measurements**
- **gas fraction in clusters is not exactly equal to the universal baryon fraction → Depletion factor, $Y_B(z)$, must be calibrated from simulations**

OTHER COSMOLOGICAL TESTS WITH GALAXY CLUSTERS

H_0 from X-ray and SZ distance measurements:

Based on a distance measuring techniques that depend on a comparison of 2 observables (Cavaliere+77):

$$E \propto \int n_e^2 dl$$

$$A \propto \int n_e dl$$

We get a standard ruler: $A^2/E \simeq \Delta L$

If the structure of the gas is known, given the angular size ϑ of the system, the angular diameter distance, $D_A = \Delta L \backslash \vartheta$, is given by:

$$D_A(z) = A^2/(E\theta)$$

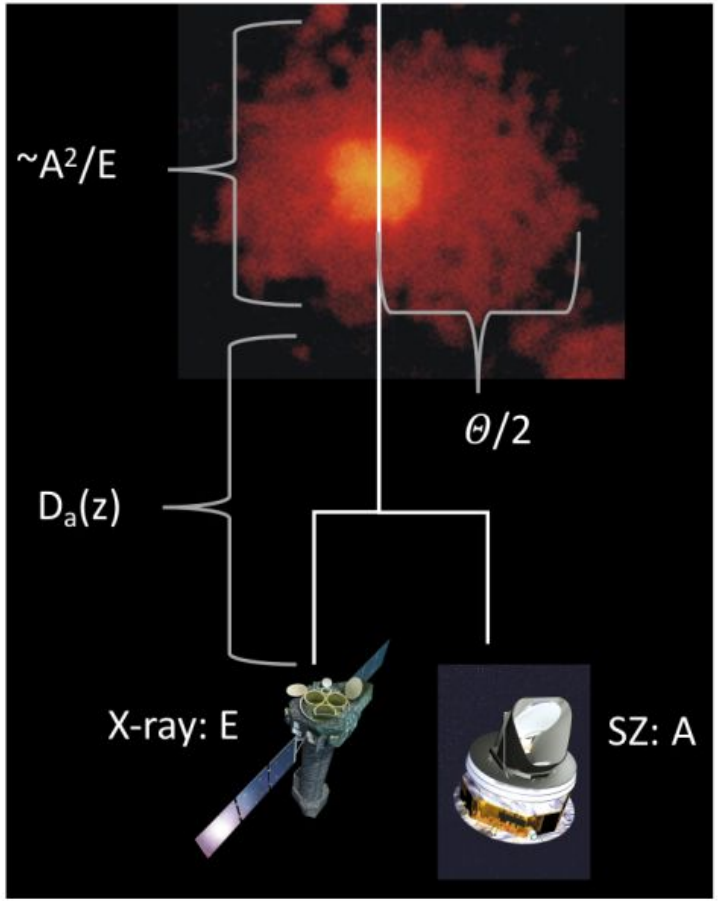

OTHER COSMOLOGICAL TESTS WITH GALAXY CLUSTERS

H_0 from X-ray and SZ distance measurements:

- Birkinshaw (1979)
- Reese et al. (2000)
- Patel et al. (2000)
- Mason et al. (2001)
- Reese et al. (2002)
- Sereno (2003)
- Udomprasert et al. (2004)
- Reese et al. (2004)
- Schmidt et al. (2004)
- Jones et al. (2005)
- Bonamente et al. (2006)
- Kozmanyan et al. (2019)

SZ measurements from RT, OVRO and BIMA, X-ray from ROSAT
26 clusters z < 0.78
H_0 = 61±3(stat.)±18(sys.) km/s/Mpc

SZ measurements from OVRO, BIMA and X-ray from Chandra
38 clusters 0.14< z< 0.89
H_0 = 76.9±4(stat.) ±9(sys.) km/s/Mpc

Three regular clusters
z=0.088, 0.2523, and 0.451
H_0 = 68±8(stat.) km/s/Mpc

SZ measurments from Planck and X-ray from XMM
61 nearby systems (z<0.5)
H_0 = 67± 3km/s/Mpc

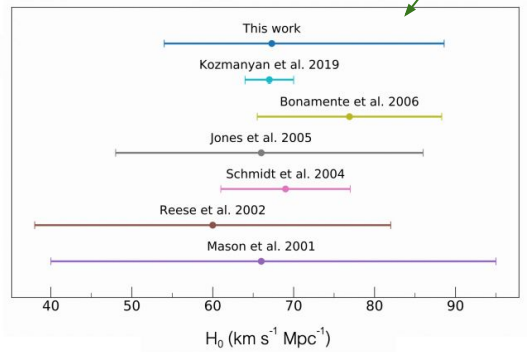

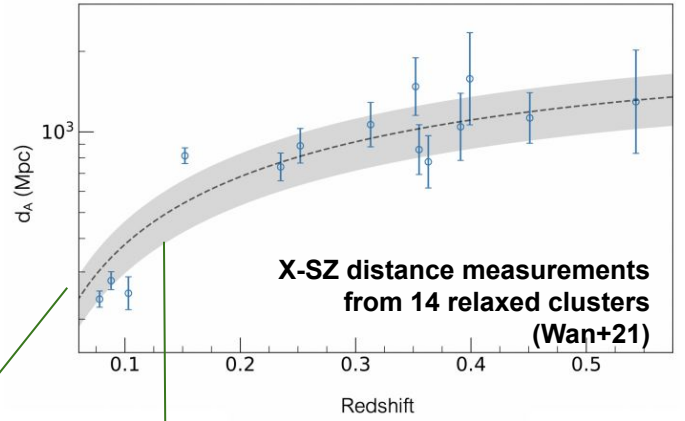

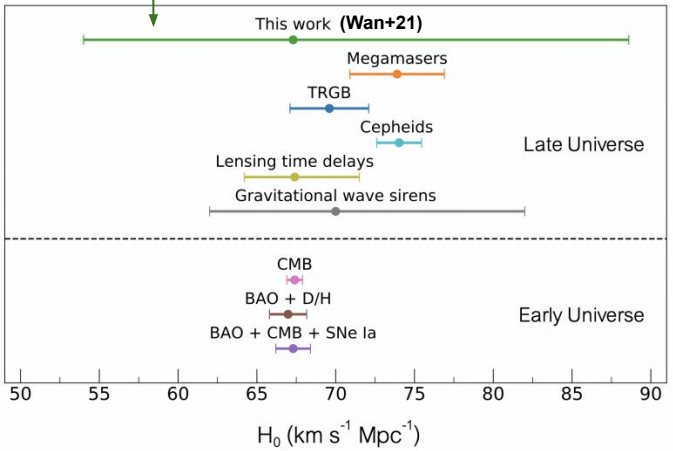

THE HALO PROFILE

From n-body/hydro simulations we can predict the dark matter/gas (spherically averaged) halo profiles. For LCDM models E.g. Navarro+97 and Einasto 1965:

$$\rho_{\rm NFW} = \frac{\rho_{\rm s}}{(r/r_{\rm s})(1+r/r_{\rm s})^2}$$

$$\rho_{\rm Ein} = \rho_{-2}\exp\left\{-\frac{2}{\alpha}\left[\left(\frac{r}{r_{-2}}\right)^{\alpha}-1\right]\right\}$$

DM halo profiles for halos of different mass and redshift

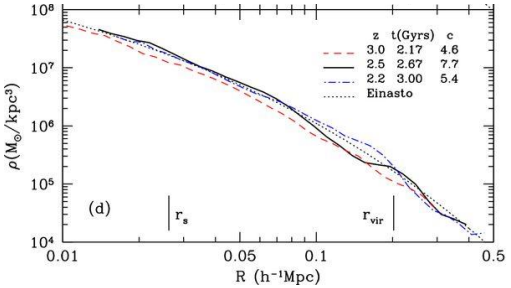

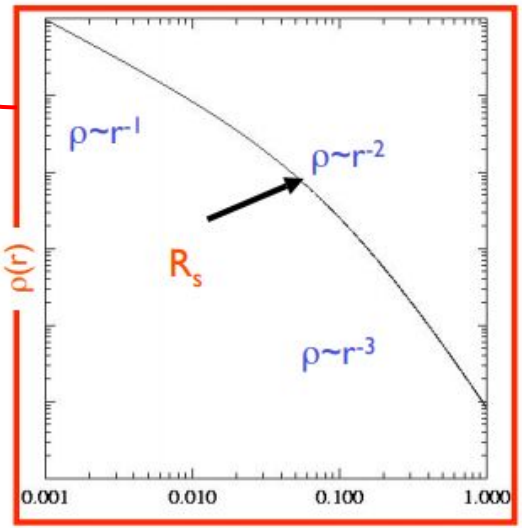

$c_{\rm NFW} = r_{200}/r_s$

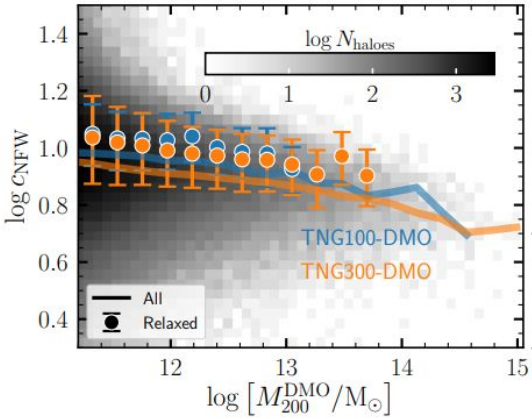

Concentration-mass relation in TNG simulation (Bose+19)

c-M primary dependence: mass and redshift →The concentration decreases with mass and redshift.

Dependence on secondary halo properties:
- Formation time and assembly history
- Halo relaxation state
- Baryonic effects

OTHER COSMOLOGICAL TESTS WITH GALAXY CLUSTERS

Cores and Self-Interacting Dark Matter (SIDM)

- A finite self-interaction cross-section leads to **heat transfer between DM particles**, transporting energy from the hotter outer regions inward and **reducing the central dark matter density** — transforming a **cusp** into a **core**
- Cross-sections of order **σ/m ~ 1 cm²/g** are sufficient to produce kpc-sized cores, consistent with observations of low-surface-brightness galaxies and dwarf galaxies
- If SIDM is universal, **cores** should exist in all dark matter halos, from dwarf galaxies to galaxy clusters — providing a **testable prediction across a wide range of scales**
- **Central DM densities in the core** regime are expected to be of order 10^7–10^8 $M_\odot$/kpc³, **significantly lower than the cusp densities predicted by collisionless CDM simulations**
- However, SIDM halos are not immune to baryonic effects: gas cooling and stellar feedback can deepen the gravitational potential and **restore a cusp-like profile**, partially erasing the SIDM core — making observational tests model-dependent

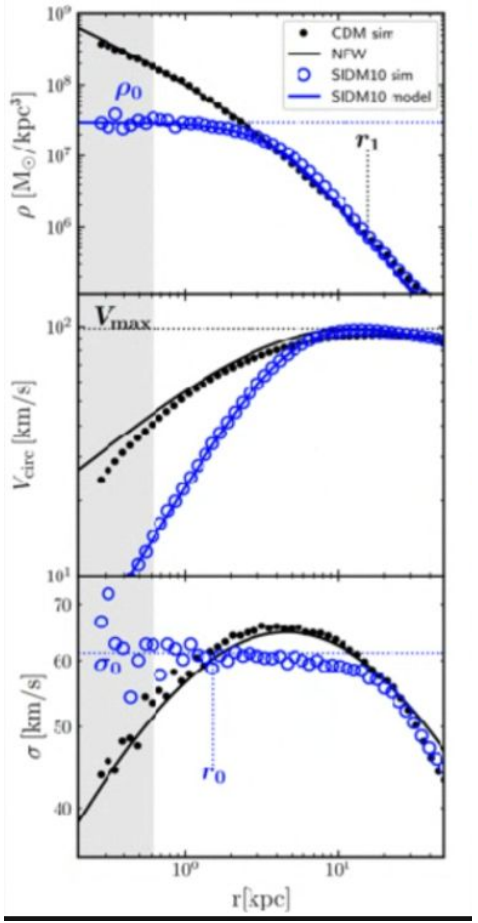

Santos-Santos 2020

OTHER COSMOLOGICAL TESTS WITH GALAXY CLUSTERS

Cores and "Fuzzy" Dark Matter (FDM)

- Fuzzy dark matter candidates have masses so small (**m ~ 10^{-22}eV**, hence the name *ultralight* axions) that their de Broglie wavelengths become comparable to the size of a **dwarf galaxy** (~1 kpc), making quantum effects relevant on astrophysical scales
- On scales smaller than the de Broglie wavelength, the quantum pressure (from the **uncertainty principle**) suppresses structure formation and prevents the density from diverging — naturally producing a central **solitonic core** instead of a cusp
- Simulations show that FDM halos develop a **soliton profile** at the centre, whose central density scales as:

$\rho_{sol} \propto m_{22}^2 \cdot M_{halo}^{4/3}$ where m_{22} is the particle mass in units of 10^{-22} eV and M_halo is the total halo mass

- Outside the solitonic core, the profile transitions to a standard **NFW-like envelope**, produced by quantum interference fluctuations that mimic granular density variations
- The soliton core size and density are therefore **fully determined by the particle mass** — making dwarf galaxy density profiles a direct probe of m_{22}

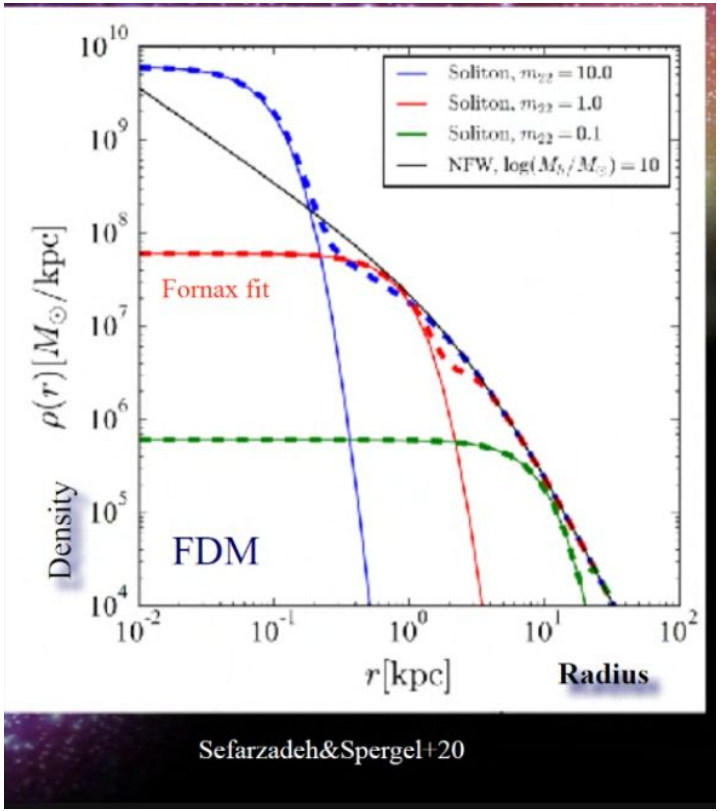

OTHER COSMOLOGICAL TESTS WITH GALAXY CLUSTERS

- **The Bullet Cluster (DM nature)**

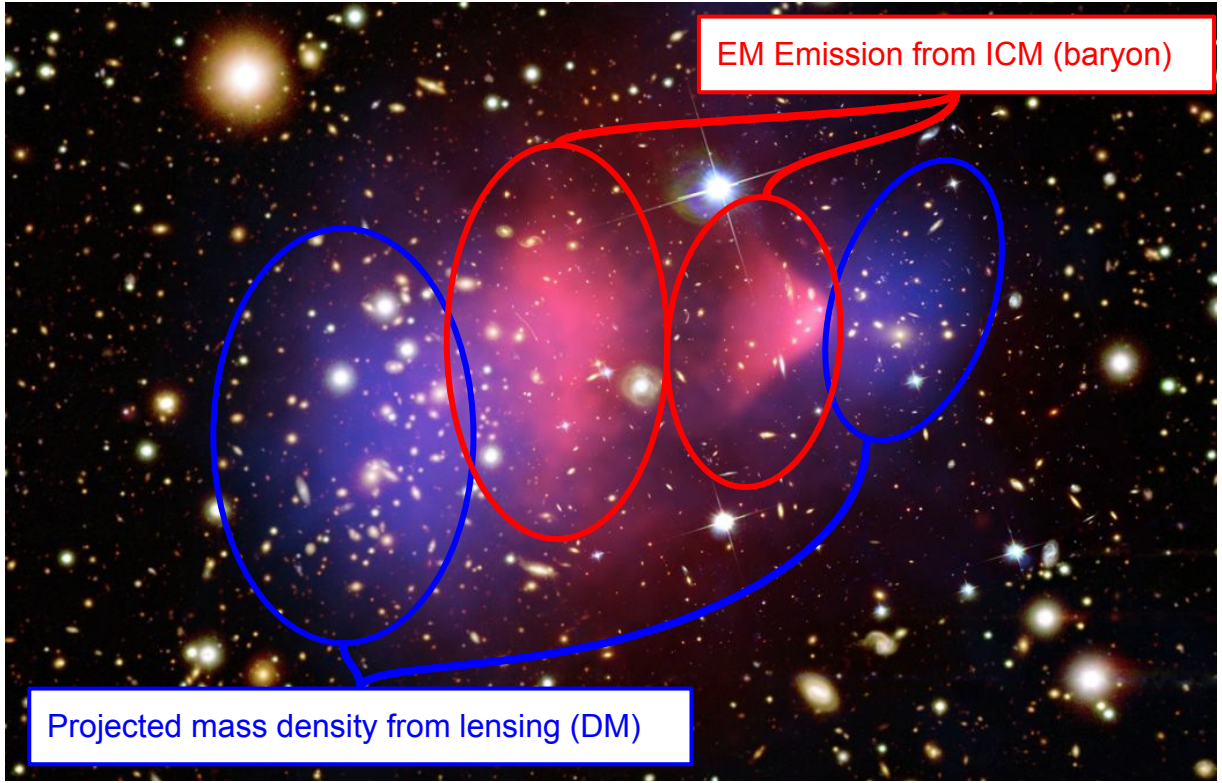

Real vs simulated Bullet-like shock (Keshet+21)

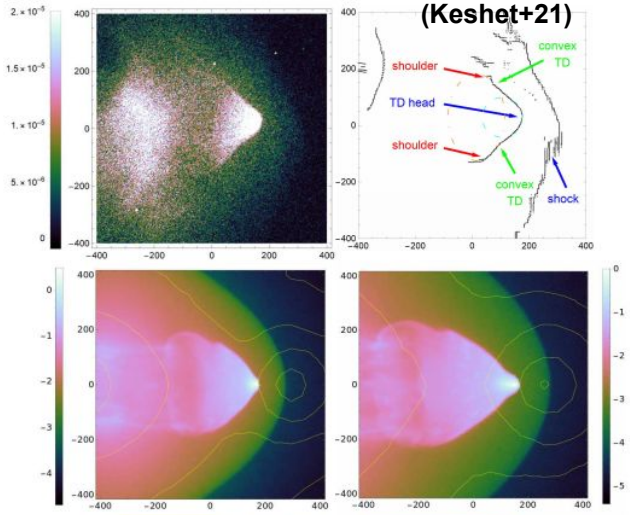

The offset between the EM and WL signal peaks, along with the shape of the shock wave, provide compelling evidence for the presence of dark matter; moreover it allows to place constraints on the dark matter cross-section

OTHER COSMOLOGICAL TESTS WITH GALAXY CLUSTERS

El Gordo (ACT-CL J0102-4915 **z=0.87, M=3 × 10^{15} $M_{\odot}$)**

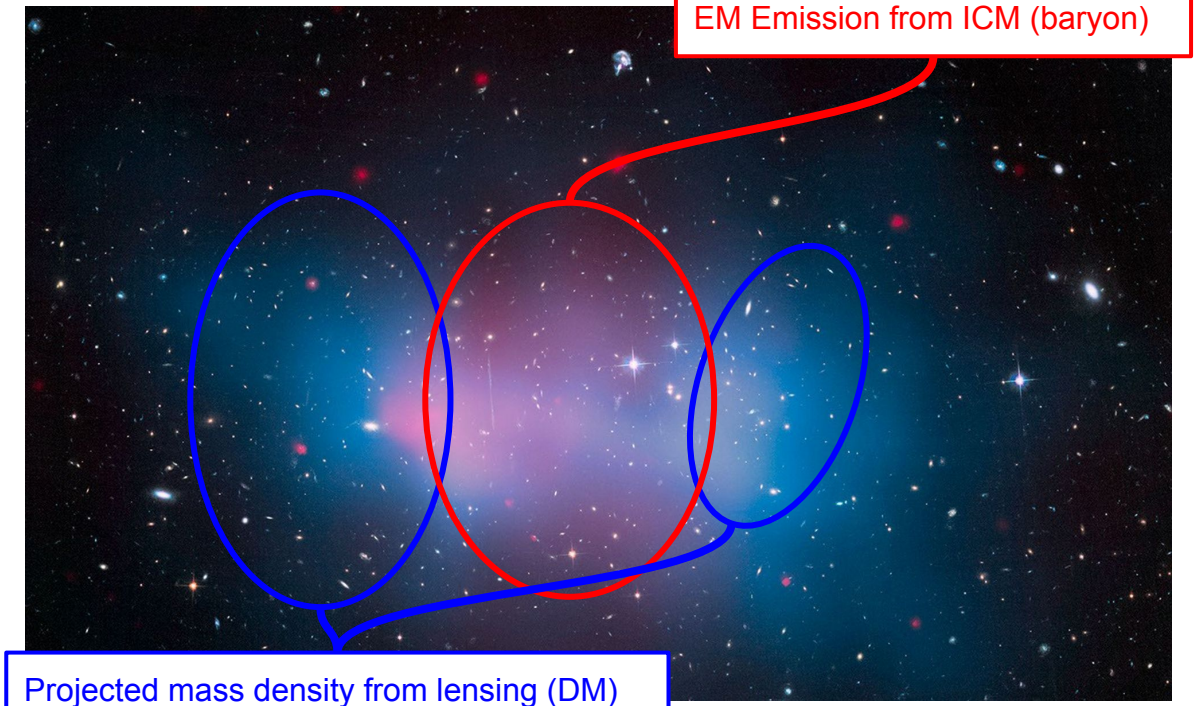

- **Systems resulting from the merger of the systems**
- **Most massive high-redshift systems**
- **Observations show significant spatial offsets between its three main components: the hot gas (X-rays), the galaxies, and the Dark Matter (detected via lensing)**

OTHER COSMOLOGICAL TESTS WITH GALAXY CLUSTERS

El Gordo (ACT-CL J0102-4915 z=0.87, M=3 × 10^{15} $M_\odot$)

DM mass density from lensing reconstruction vs simulation output [Valdarnini 2025]

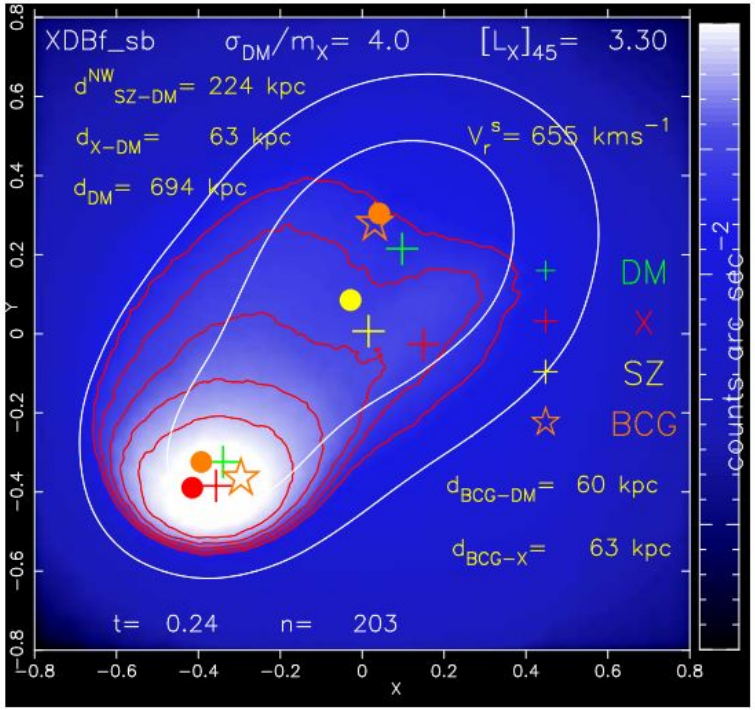

- **Self Interacting DM:** A cross-section of σ_{DM}/m_X ~ 4-5 cm^2/g successfully reproduces the observed offsets between galaxies and Dark Matter.
- However, this level of interaction causes the Dark Matter halos to develop **"cores"** (flat density centers) rather than the "**cusps**" (sharp peaks) predicted by standard NFW models and seen in observation.

DM density profiles of NW and SE subclusters — data points from lensing, curves from NFW (dashed) and cored (solid) models"

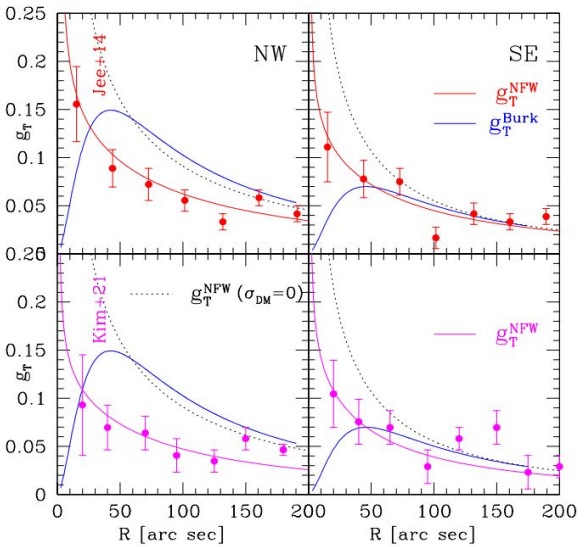

OTHER COSMOLOGICAL TESTS WITH GALAXY CLUSTERS

Mass estimates from accretion shocks https://arxiv.org/abs/2407.01660: Utilizing a sample of simulated galaxy clusters the analysis reveals that these clusters lie on a well-defined plane within the three-dimensional space defined by mass (M), shock radius (R_s), and Mach number $\mathscr{M}$ (indicating shock strength). This planar relationship suggests a predictable correlation among these parameters.

$$\log_{10}\frac{M(<2R_{\rm vir})}{M_\odot} = 12.760 + 1.910\log_{10}\frac{R_{\rm sh}}{\rm Mpc} + 0.0117\mathscr{M}_{\rm sh}, \qquad (\text{at } z=0)$$

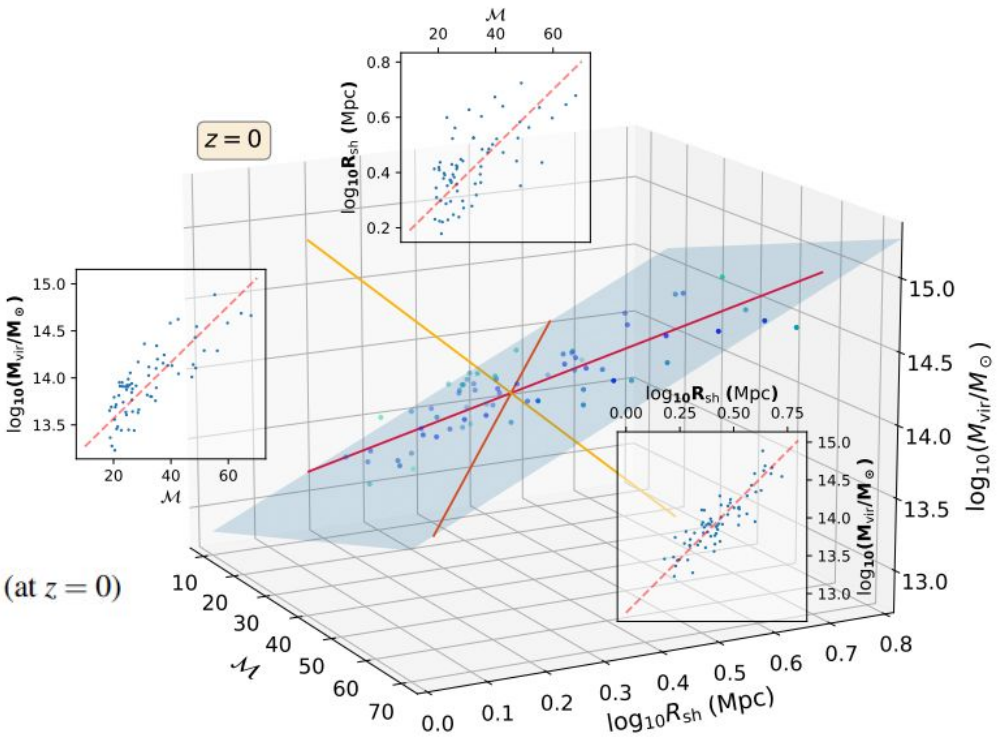

OTHER COSMOLOGICAL TESTS WITH GALAXY CLUSTERS

- **Galaxy cluster mass profile:**

The shape/slope of the halo profile, especially in the inner regions, can be used to test several fundamental physics model, such as the nature of dark matter (e.g. warm vs cold, interacting DM) or GR test.

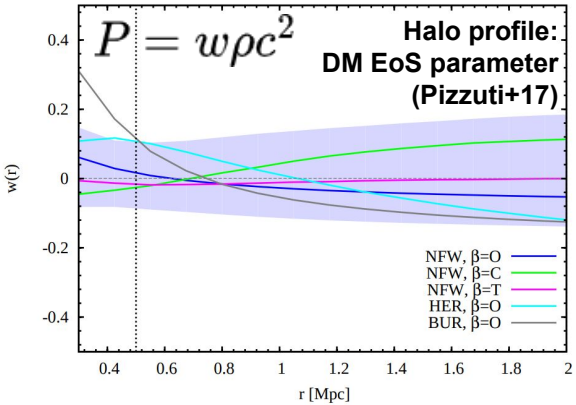

Halo profile: Interacting DM vs DM (Vega-Ferrero+20)

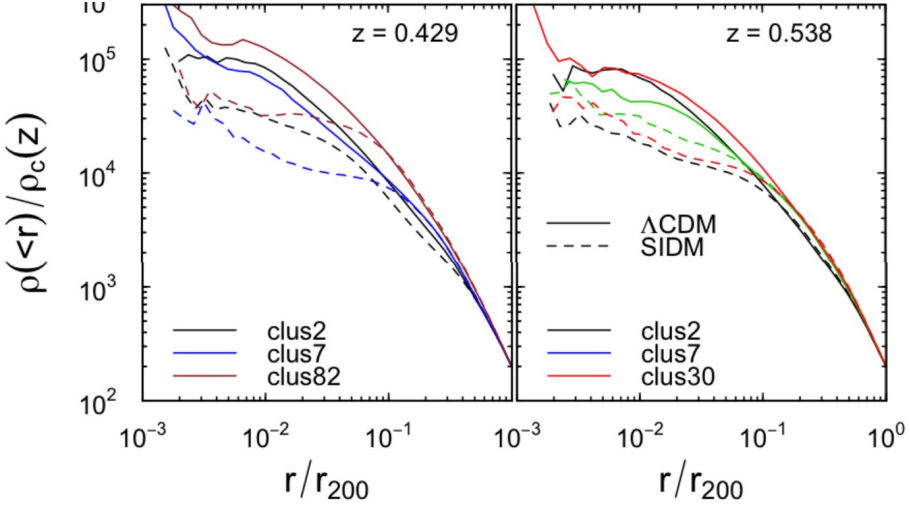

Halo profile: f(R) constraints (Butt+25)

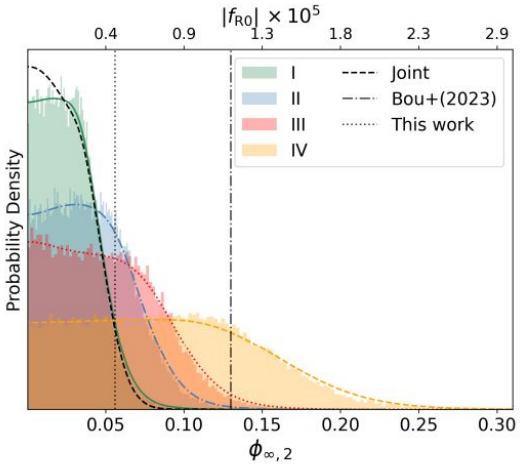

OTHER COSMOLOGICAL TESTS WITH GALAXY CLUSTERS

Constraining deviation from GR with the mass profiles (Pizzuti et al 2025):

- Compare mass profiles reconstructed from lensing and kinematic data to constrain the anisotropic stress parameter $\eta = \psi / \phi$ (GR: $\eta = 1$)
- **Gravitational Lensing:** Sensitive to the sum of the potentials ($\phi + \psi$)
- **Galaxy Kinematics (Dynamics):** Sensitive only to the temporal potential (ψ)

$$\eta(r) = \frac{\int_r^\infty \left[2M_{\rm lens}(r') - M_{\rm dyn}(r')\right] \frac{{\rm d}r'}{r'^2}}{\int_r^\infty M_{\rm dyn}(r') \frac{{\rm d}r'}{r'^2}} .$$

Constraints on η from 9 massive cluster from CLASH-VLT sample

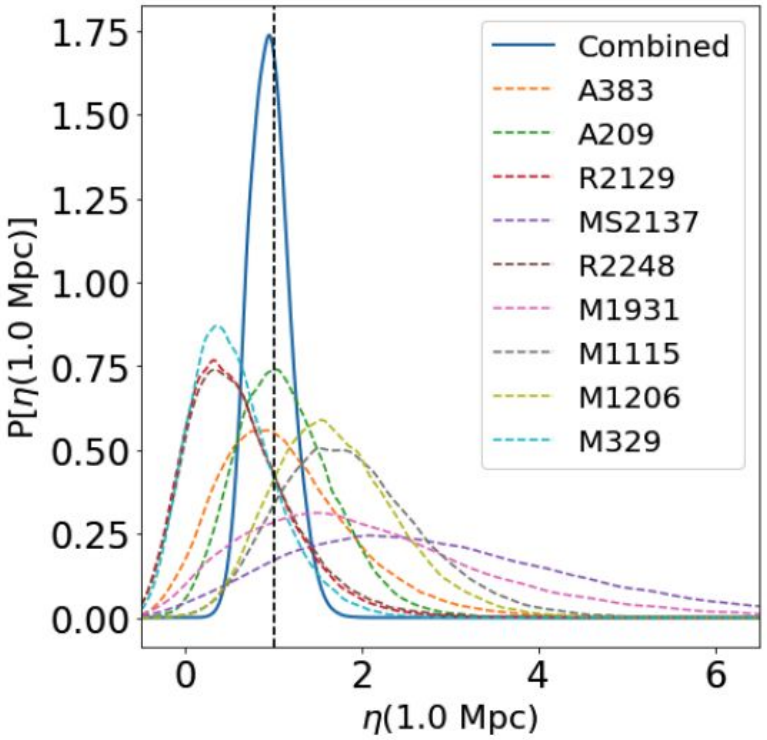

OTHER COSMOLOGICAL TESTS WITH GALAXY CLUSTERS

Gravitational redshift in galaxy clusters:
Light escaping a gravitational potential well is redshifted:
$z_{gr} = \nabla\Phi / c^2$
For cluster masses ~10^{14} $M_\odot$ → cz_{gr} **≈ 10 km/s << Doppler broadening (~1000 km/s)**

Galaxies near the cluster centre sit deeper in the potential well and are more redshifted, so the GR velocity shift Δ(R) is most negative at small R and rises (less negative) toward the outskirts. In the rest frame of the brightest cluster galaxy (BCG), this manifests as a systematic blueshift of the velocity distribution centroid

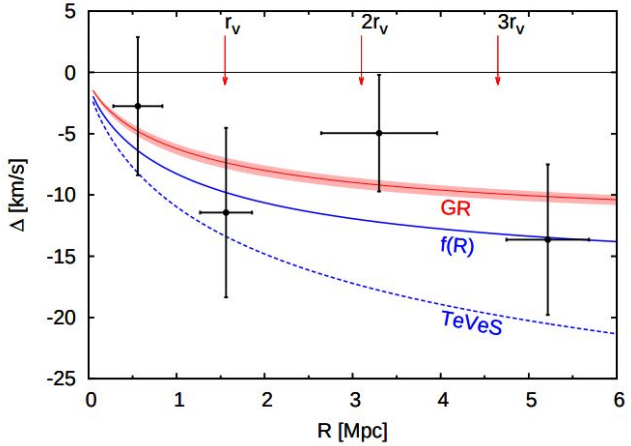

(Wojtak et al. 2011)
gravitational redshift shifts the **centroid** of the velocity distribution; Doppler only broadens it symmetrically.
- **7,800** SDSS galaxy clusters (DR7)
- Stacked to average out Doppler noise
- Velocity distributions measured in **4 radial bins** (0–6 Mpc)
- BCG used as cluster center & rest frame

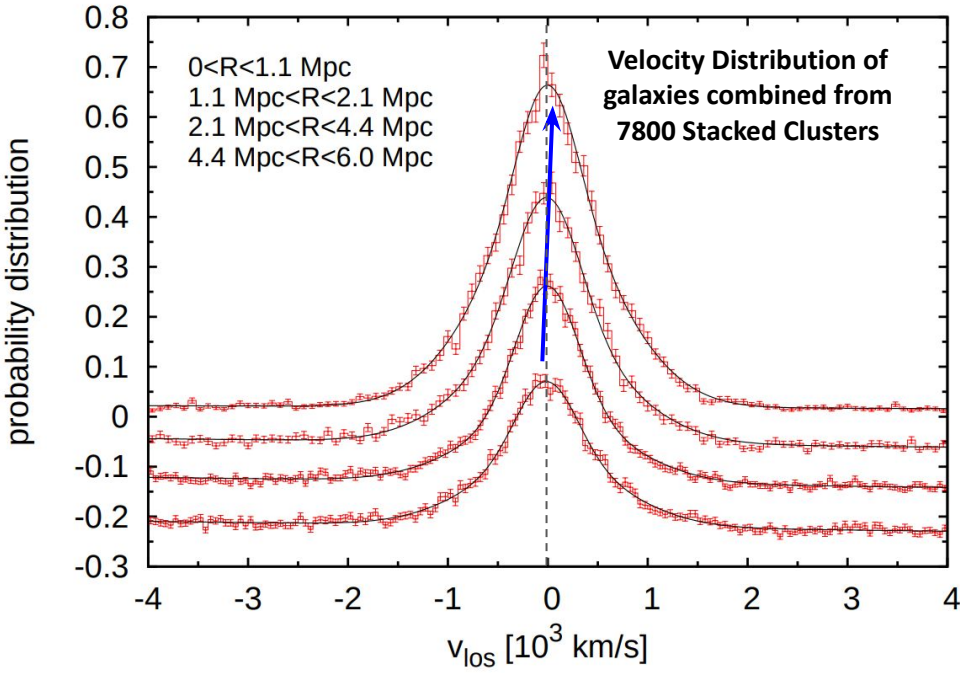

See Di Dio et al 2025 for a complete treatment of the effect